Technical Note

1969-18

J. E. Evans

Preliminary Analysis of ELF Noise

26 March 1969

Lincoln Laboratory

MASSACHUSETTS INSTITUTE OF TECHNOLOGY

Lexington, Massachusetts

AD691814

MASSACHUSETTS INSTITUTE OF TECHNOLOGY

LINCOLN LABORATORY

PRELIMINARY ANALYSIS OF ELF NOISE

J. E. EVANS

Group 66

TECHNICAL NOTE 1969-18

26 MARCH 1969

LEXINGTON   MASSACHUSETTS

ABSTRACT

Preliminary results of analyzing extremely low frequency (ELF) electromagnetic noise recorded in Florida and Malta are presented. The results include wideband waveforms, power density spectra, amplitude probability distributions and probability distributions for the duration of the interval between noise bursts. The distinctly non-Gaussian nature of the noise is demonstrated in a variety of ways.

PRELIMINARY ANALYSIS OF ELF NOISE

I. INTRODUCTION

Electromagnetic noise in the ELF frequency band (1 - 300 Hz) is primarily generated by lightning strokes propagating in the earth-ionosphere cavity. The low attenuation rate that arises from this mode of propagation means that the noise level at a given location can be significantly affected by thunderstorms (i.e., lightning strokes) hundreds of miles away.

In this report we,

(1) present some preliminary results of the analysis of wideband 0 to 300 Hz) ELF noise recorded by Lincoln Laboratory [1] in Florida during 1968;

(2) discuss the approach toward noise analysis that has evolved to date.

The distinctly non-Gaussian nature of the wideband noise process is clearly demonstrated. The preliminary noise analysis is discussed in the context of developing a mathematical model for the noise process based on the first and second order statistics. Finally we describe some results of analysis oriented toward developing a model that more explicitly takes into account the large spikes (due to lightning strokes) that characterize the wideband process. The effort in this area has focused on obtaining a statistical description of both the arrival times between spikes and the time duration of a given spike.

II. DATA ANALYSIS

In Fig. 2-1, we indicate the overall structure of the noise processing at Lincoln Laboratory. The raw noise data are recorded wideband (approximately 3 to 300 Hz) and put into digital form by use of an A/D converter; all further processing takes place on the Lincoln Laboratory 360 computer. A first step is processing the wideband noise to yield noise

amplitude distributions and spectra. The recorded noise represents the result of passing the actual noise through an antenna, recording system, etc. Equalization is necessary to remove the effects of this processing. Finally, we obtain the statistical characteristics for the equalized noise.

Next, we discuss some details of the methods used to obtain the various statistical characteristics of the data. The computer program which obtains estimates of the spectral density of the noise process uses a form of the direct method known as the "direct segment" method. [2, 3] In the direct method of spectral analysis, the data is transformed immediately in the frequency domain and then the spectrum is computed from the transformed data. The "direct segment" method obtains the spectra by the following steps:

(1)   for each sensor, the sampled data values which are to be used in the estimation are divided into a number of smaller groups, each representing a continuous segment of the process.

(2)   the data in each segment for each sensor is transformed to the frequency domain and these transforms are then used to obtain an estimate of the spectrum for each sensor and the cross spectrum between selected pairs of sensors (these spectra and cross spectra estimates are called the modified periodogram and modified cross periodogram respectively). [3]

(3)   the stability of the spectra and cross spectra estimates is then increased by averaging over the spectra and cross spectra for various segments.

The three criteria most frequently used to judge the merits of a spectra estimation procedure are:

(1)   the bias of the estimate
(2)   the variance of the estimate
(3)   the amount of computer time required to obtain the estimate.

Capon, et. al [2] have examined these issues in considerable detail and conclude that the approach utilized here yields approximately the same bias and

2

variance as other approaches, in addition to requiring considerably less computer time. Furthermore, and perhaps most importantly for ELF noise spectra estimation, the "direct segment" method allows us to test for and measure nonstationarity (i.e., a spectrum which is slowly changing with time) by examining differences between the spectral estimates for different segments.

The method by which the data is transformed to the frequency domain deserves some discussion in so far as it reflects on the bias and the amount of computer time required. The transform of the noise data $x_j(t)$ in the nth segment; j^{th} sensor and frequency w_k is

$$X_{jn}(w_k) = \sum_{m=1}^{N} w(m) \; x_j [m T + (n-1)NT] \; e^{jmw_k T} \qquad (II-1)$$

where; $w(m)$ = a weighting function used to reduce the bias due to spectral sidelobes. [6]

N = the number of sample values of $x(t)$ used per segment.

$x_j [m T + (n-1)NT]$ = the value of $x_j(t)$ at time $t = mT + (n-1)NT$

T = the sampling interval.

The $X_{jn}(w_k)$ are computed for $w_k = 2\pi k(\frac{1}{T})$ $k = 0, 1, \ldots N$ using the Fast Fourier Transform (FFT). Typically N is on the order of 1024 - 2048 (corresponding to a data segment 1 - 2 seconds long). The use of the FFT algorithm reduces the computation time by approximately 100 times over that used by previous investigations of ELF noise. [4]

The estimate of the spectral density at frequency w for the jth channel is taken to be:

$$S_j(w) = \frac{1}{MNT} \sum_{n=1}^{M} \frac{1}{U} \left| X_{jn}(w) \right|^2 \qquad (II-2)$$

3

where; M = number of segments we average over

$$U = \frac{1}{N} \sum_{m=1}^{N} [w(m)]^2.$$

It can be shown that the estimate defined by II-2 is equivalent to computing the power at the output of a linear filter and dividing by the filter bandwidth. Thus our estimate of the density at frequency w represents an average of the power at frequencies in the passband of the equivalent digital filter. In Fig. 2-2 we show a plot of the frequency response of the filter defined by equation II-2 for the w(m) used here

$$[w(m) = 1 - \left| \frac{m - \frac{N}{2}}{\frac{N}{2} + 1} \right| \quad \text{which is known as a } 1 - |t| \text{ window}].$$

Bias in the estimate of $S_j(w)$ is primarily caused by large spectral components at a side-lobe of the spectrum. As can be seen from Fig. 2-2, the nearest side lobe has a level of 26 dB down with the higher order side lobes over 55 dB down.

Stability of the spectral estimates for ELF noise is somewhat difficult to establish a priori since the measurements to date of narrowband statistics were at wider bandwidths than those used here. One can use tabulated results[5] for the variance of spectral estimates of a Gaussian process as a lower bound on the expected variations of the spectra. The spectra considered in this report were obtained by averaging over 50 segments, which yields a 90% confidence limit of ± 1 dB if the process were stationary and Gaussian.

The particular amplitude probability distributions obtained for the ELF noise are:

      (1)   the sample probability density function, $\tilde{p}(x)$

      (2)   an estimate of the ensemble probability density function

based on $\widetilde{p}(x)$ (the method by which this estimate is obtained will be described in a separate report)

(3) the sample exceedance probability $\widetilde{P}_{ex}(x)$.

The functions $\widetilde{p}(x)$ and $\widetilde{P}_{ex}(x)$ are estimated as follows:

$$\widetilde{p}(x) = \frac{1}{\delta} \; [\text{fraction of noise samples in range } (x - \frac{\delta}{2}, \; x + \frac{\delta}{2})]$$

$$\widetilde{P}_{ex}(x) = \text{fraction of noise samples having values} \geq x.$$

where δ is typically $.05 \; \sigma_x$ (σ_x = standard deviation of x).

The statistical properties of $\widetilde{p}(x)$ will be discussed thoroughly in the report mentioned above, so we will confine our discussion of estimate bias and variance to $\widetilde{P}_{ex}(x)$. It can be shown that if the N noise samples of the process used in obtaining $P_{ex}(x)$ are statistically independent and all drawn from an ensemble whose ensemble, i.e., "true" exceedance is $P_{ex}(x)$, then

$$E \; [\widetilde{P}_{ex}(x)] = P_{ex}(x) \tag{II-3}$$

and

$$\text{Var} \; [\widetilde{P}_{ex}(x)] = (\frac{1}{N}) \; P_{ex}(x) \; [1 - P_{ex}(x)]$$

A useful measure of the reliability of the estimate $\widetilde{P}_{ex}(x)$ is the ratio

$$R = \frac{\sqrt{\text{Var}[\widetilde{P}_{ex}(x)]}}{E[\widetilde{P}_{ex}(x)]} = \frac{\sqrt{1 - P_{ex}(x)}}{\sqrt{N P_{ex}(x)}} \quad . \tag{II-4}$$

In general, we would like $R < \frac{1}{4}$, so that we find for a given N, the smallest $P_{ex}(x)$ that we would expect to "reliably" estimate is

$$P_{ex}(x) \approx \frac{16}{N} \quad . \tag{II-5}$$

In practice, the samples used are not statistically independent, and

there is no simple way to quantitatively estimate the effects of the lack of independence. One indication of the degree of independence is the normalized auto-correlation function

$$\varphi(\tau) = \frac{E[x(t)x(t+\tau)]}{Var[x(t)]}$$

considered as a function of τ. For the wideband (i.e., 2 - 300 Hz) noise analyzed to date, it seems that $\varphi(\tau)$ goes to zero when $|\tau|$ is of a duration corresponding to 3 - 5 samples. This suggests that one probably should multiply N in equation II-5 by an additional factor (e.g., 1/2 or 1/3 to take into account the statistical dependence between the samples.

In Fig. 2-3 we show the raw power spectrum density for a wideband tape recorded in Florida in February 1968. The spectral lines at multiples of 60 Hz presumably are due to power lines near the recording site. The equalization process removes these lines and low-pass filters the data to approximately 250 Hz using a linear phase digital filter developed at Lincoln Laboratory. (This filter will be described in a later report.)

Because of the difficulty of locating recording sites completely free of power-line radiation of the type shown in Fig. 2-3, a subject of considerable interest is the amount of power-line components that can be tolerated. In terms of the spectra of the ELF noise, one can assume that the ELF noise spectra are reasonable smooth and thus can estimate the ELF spectra at the power-line frequencies by examination of the spectra adjacent to the power frequencies. From the viewpoint of spectral analysis alone, a power-line component as much as 50 dB above the nearby ELF density will not bias the spectrum significantly, provided that a suitable spectral window is used.

The next issue that arises is the effect on the APD of ELF noise of notch filtering and low-pass filtering. A segment of data recorded in Florida in May 1968 had a 60-Hz component corresponding to a power 23 dB below the ELF noise power (the 60-Hz rms level was 0.067 of the rms of the ELF noise) and no other noticeable power-line components. The APD's before

and after applying a filter with notches at 60 and 180 Hz and a passband from 0 - 300 Hz were compared, and virtually no difference was found either in the behavior for small values of the input or in the behavior for large values of the input (i.e., on the tails). Hence, we assume that the notch filtering and low-pass filtering do not significantly change the properties of the ELF noise process.

Next, we consider the point at which the power-line component seems to significantly affect the APD. We find that this point lies somewhere between the two cases below:

	Total Power in Power-Line Components (dB re ELF power less power-line components	Power in Largest Power-Line Component (dB re ELF power less power-line components
Little or no effect	- 8.6	- 10.0
	- 1.1	- 1.5

Finally, we consider how large the power-line content may be before usable data cannot be obtained by appropriate filtering. Data recorded in New Hampshire in March 1968 had power-line components whose sum power was 14.7 dB above the ELF noise power to 180 Hz (the most prominent power-line component had a power 13.7 dB above the ELF noise power). The APD after filtering was qualitatively quite similar to the results of filtering Florida data (which had far smaller power-line components) to the same bandwidth and also qualitatively similar to the APD of Florida data before filtering. Thus, it appears that useful information can be obtained in cases where significant power-line components are present, although we have not yet set an upper bound on allowable power-line levels.

III. NOISE WAVEFORMS

In Fig. 3-1, we show a sample of the wideband noise recorded in Florida during January 1968. This particular sample corresponds to an absolute noise level at 50 Hz of -131 dB with respect to (wrt) 1 amp/meter/$\sqrt{Hz}$; i.e., a low level noise sample. In Figs. 3-2 and 3-3, we show samples of wideband noise recorded in Florida during high local thunderstorm activity period in June and July. The June sample corresponds to an absolute noise level of -111 dB wrt $1A/m/\sqrt{Hz}$; i.e., a very high level noise sample.

By (careful) examination of the various waveforms on the loops (and whip), one can ascertain information regarding the location of thunderstorm sources with respect to the measurement site. In both cases, there seem to be sources that lie largely in the plane of one of the loop antennas; i.e., sources almost directly east (and/or west) and almost directly south (and/or north) of the receiver.

The tendency for spikes to be followed by another spike approximately 50 msec later is thought to be due to the physical mechanism of spike production. A single spike arises from the fields generated by a single lightning stroke. Several "return strokes" occurring 50 msec apart may accompany a main stroke, thus generating a sequence of spikes. In Fig. 3-4 we show a sample of the wideband noise from February together with the traces that result from passing the wideband noise through 3-Hz filters centered at various frequencies. The effect of the large spikes is clearly exhibited in these other traces. It should be pointed out that a Gaussian noise process would not exhibit the dependence visible here between the noise components at various frequencies. Thus, in Fig. 3-4, we have a dramatic demonstration from the viewpoint of spectral decomposition that the wideband ELF noise is not Gaussian.

In a program where the bulk of data recording and analysis has been performed on data from a single geographic location but the region of interest is global, one is interested in the nature of wideband waveforms at

other locations. In Fig. 3-5 we show a sample of wideband noise recorded in Malta in October 1968. This particular sample corresponds to a noise level of -130 dB wrt $1A/m/\sqrt{Hz}$; i.e., a level quite close to that for the Florida February noise sample. In Fig. 3-6 we show a sample of wideband noise recorded in New Hampshire in March, 1968.

The loop waveforms shown in Figs. 3-1 to 3-6 represent the H field waveform after passing through the loop (which yields the time derivative of the H field waveform as its output) and the various system amplifiers. In Fig. 3-7 we show the waveforms that resulted from passing the loop data through a filter whose filter frequency response from 10 - 300 Hz is the inverse of the filter frequency response for the cascade of the loop and system amplifiers.

IV.   POWER DENSITY SPECTRA

The wideband power density spectrum is of interest because (as indicated in the previous section) the ELF noise in one frequency band is, in general, correlated with noise in other frequency bands. Thus, we are interested in the relationship of the out-of-band noise to the inband noise at the same instant of time.[*] The method of spectral analysis described in Section II obtains an estimate of the density at all frequencies of interest (i.e., from 0 Hz to 500 Hz (= 1/2 sampling rate)) from the same data so that we can directly compare the spectrum levels to determine if, for example, changes in the power at various frequencies are correlated. Also, of course, one is interested in the values of the spectrum expressed in absolute quantities.

In Figs. 4-1 and 4-2, we show wideband noise spectra (corrected for recording system response) for high level noise days in June and July 1968 respectively. The large amount of energy from 4 - 15 Hz on the July tape presumably is due to motion of the antenna caused by the wind (there was a nearby thunderstorm). In Fig. 4-3 we show representative (corrected) spectra (including the highest level for each month) for data recorded during February, May, June and July.

In Fig. 4-4, we show the raw spectra for June in order to see how the change in power level at one frequency is related to changes in power level at other frequencies. From Fig. 4-4 (and other data not shown here), it appears that the ELF spectra at high noise levels are the same to within a

---

[*] It should be noted that most previous (and ongoing) measurements of wideband ELF spectra are not very helpful in this respect for a variety of reasons:

1.   the power at various frequencies is obtained from different portions of data, so that one must assume spectral stationarity of the process to an extent that may not be justified. [11]

2.   the power is measured at a very small number of frequencies, and one must interpolate somewhat arbitrarily between frequencies to estimate the complete density. [4, 11]

3.   the spectra were obtained over a small portion of the frequency range of interest. [4, 8, 9, 13]

multiplicative constant, i.e.,

$$S(f, T_1) = k S(f, T_2) \qquad \text{(IV-1)}$$

Thus, given knowledge of the entire spectrum for one period, one can predict the entire spectrum at a new time given knowledge of the spectrum at a single frequency of the new time.

A conspicuous exception to IV-1 occurs at low frequencies in periods of rather low noise level. In Fig. 4-5, we show the corrected and uncorrected spectra density for a low noise period in February 1968. The peaks in the spectra at 8, 14 and 21 Hz are caused by resonances of the earth-ionosphere cavity, i.e., the Schumann resonances (so named because Schumann [16] predicted their existence theoretically before they were measured). These were first measured experimentally by workers at Lincoln Laboratory [6, 7] and have since been studied by a number of investigators. [8-9, 12-13, 15, 17] To date, we have studied the properties of these resonances only cursorily as we have observed them only at low noise levels.

Another characterization of a random process closely related to the power density spectrum is the auto-correlation function (for stationary ergodic processes, the auto-correlation function and power density spectrum are a Fourier transform pair). In Fig. 4-6, we show the normalized auto-correlation function[*]

$$\varphi(\tau) = \frac{E[x(t)\ x(t+\tau)]}{\text{Var } [x(t)]}$$

for a sample of noise recorded in June after the power line frequencies have been removed and

(1)   the noise filtered to produce a spectrum that is constant over the passband.

(2)   the noise filtered to produce a noise process corresponding to the H field at the loop (i.e., put through the inverse filter for the antenna and amplifier electronics).

---

[*] $E[x(t)] = 0$

11

V.   NOISE AMPLITUDE STATISTICS

The noise amplitude statistics are of interest for several reasons:

(1)   they give some useful information toward describing the wideband noise process. For example, if the wideband noise process had a Gaussian probability density function, one could then apply the large amount of available knowledge regarding Gaussian noise to develop appropriate mathematic models. Unfortunately, as we shall show, the wideband ELF noise amplitude statistics are distinctly non-Gaussian and so we must consider a more general model for the noise.

(2)   for the case where the noise process is sampled such that successive noise samples are identically distributed statistically independent random variables, the sampled noise process can be completely characterized by either its probability density function or its exceedance probability.

(3)   for the case where the successive samples are not statistically independent, the first order noise amplitude statistics provide information that may be useful in developing a model.

In Figs. 5-1 and 5-2 we show the sample probability density function and sample exceedance probability for wideband data corresponding to high, medium and low noise levels. In Fig. 5-2 we have plotted the exceedance probabilities in standard deviation units (i.e., rms units) from the mean so that we may compare the exceedance probability for Gaussian noise of the same level. We note that the ELF noise is characterized by much slower tails, i.e., large values are far more probable for ELF noise than for Gaussian noise of the same level.

Another way to demonstrate the slow tails of the wideband ELF process as compared to a Gaussian process is shown in Fig. 5-3 where we plot the fraction of noise power corresponding to absolute values ≥ a given noise amplitude in rms units. We see that for Gaussian noise, only .1% of the noise power corresponds to amplitudes above 4 rms units where as for the

12

ELF noise data, approximately 80% of the noise power corresponds to amplitudes above 4 rms units.

The data shown in Figs. 5-1 and 5-2 represents the noise amplitude statistics for the noise process as recorded on the analog tapes before any equalization. In Fig. 5-4 we show the sample exceedance probability (SEP) for data from a high noise level period in June as recorded as well as the SEP for the same data after:

(1)   filtering to remove power lines and to give a passband from 10 - 300 Hz;

(2)   filtering to produce a spectra that was constant from 10 - 300 Hz and in which the phase distortion due to the loop antenna was removed;

(3)   filtering to remove the amplitude and phase distortion due the antenna and amplifiers from 10 - 300 Hz.

From Fig. 5-4, we see that the exceedance probability for the various forms of the wideband process are not very different qualitatively.

In Fig. 3-2, we saw that the waveforms on the E field sensor (i.e., the whip) were severely distorted during periods of high noise levels because of the environmental conditions. In view of the experimental problems in recording the whip data, we have been primarily concerned with analysis of the loop data. A question that naturally arises is the degree of statistical similarity between the loop and whip data for periods when the whip data was recorded satisfactorily. In Fig. 5-5, we plot the exceedance probability for the two loop channels and a whip for a period in February with a noise level of -131 dB wrt $1 A/M/\sqrt{Hz}$ at 50 Hz (i.e., a low noise level). We see that the exceedance probability has virtually the same form for all three sensors.

In Fig. 5-6 we show the exceedance probability for a sample of high noise level data from June as a function of the bandwidth of the process (linear phase) digital filters with passband gains of 1.0 were applied to the wideband data to give the noise processes from which we obtain the data for

Fig. 5-6. The exceedance probability of the envelope of the narrow band ELF process is also of interest because other investigators have measured this. In Fig. 5-7 we plot the exceedance probability for some data from February. We see that the exceedance probability is Rayleigh for small values, but decreases more slowly than a Rayleigh process for large field values. This behavior is quite similar to that obtained by other investigators. [13-15, 17-18]

Another topic of interest is the differences between the statistics for data at high noise levels. In Fig. 5-8 we plot the exceedance probability for several segments of data recorded during high noise levels in June. From Fig. 5-8 we do not see any clear correlation between spectral level and the tails of the exceedance probability.

In Fig. 5-9 we show the exceedance probability for data recorded in Malta in October, 1968. We note that Fig. 5-9 is quite similar to the Florida data shown in Figs. 5-2 and 5-8. In Fig. 5-10 we plot the exceedance probability for various data from Malta and Florida.

VI.   STUDIES TOWARD A MORE COMPLICATED MODEL FOR ELF NOISE

Next we wish to consider a more complicated model for the ELF noise process that will at least in part account for the physical origin of the noise.   From Section III, it is clear that the most prominent feature of the noise is the large spikes which seem to occur in a haphazard way in time. This suggests a model in which the observed noise is the sum of a random pulse process (corresponding to the lightening strokes) and a background process.

Such models have been proposed and analyzed in part by Beckmann, [18] and Furutsu and Ishida. [19] In all these cases, the model proposed (in the case of the ELF band) suggests that the received noise consists of the sum of a pulse process and Gaussian noise.   The pulse process is generated by having a Poisson impulse process (i. e. , a series of impulses that are Poisson distributed in time) excite a fixed filter with the strength of each impulse being random.

Here we will discuss analysis to date oriented toward determining the appropriateness of a model in which the observed noise is the sum of a pulse process and a background process.   We have focused our attention on analyzing the pulse process as a series of point events in time.   The particular point events that we have chosen to investigate are the "beginning" and "end" respectively of the pulses (the criteria by which "beginning" and "end" are defined will be discussed in detail later).   This choice of point events leads one into a consideration of statistical characteristics of the intervals between pulses and the duration of a pulse.

The results given here are primarily concerned with characterizing the probability density functions of the intervals between bursts and the duration of a burst.   However, we will present some preliminary results of an investigation to determine if the intervals between events are independent identically distributed random variables.

Establishing a suitable quantitative criteria for the presence of a pulse in wideband ELF noise is much more difficult than determining pulse presence in the envelope of narrowband ELF noise [20], as can be seen by inspection of the waveforms in Figs. 3-1 to 3-6. In Fig. 6-1 we show the particular criteria we have used to define a pulse. These criteria have been established on a somewhat arbitrary basis. However, as we shall show, the results to date do not seem to be very sensitive qualitatively to the particular relationship of various parameters.

There are a variety of statistics one may consider in characterizing the process of pulses. The most common of these are:

(1) the mean interval at various values of T_L, T_u and S_c

(2) the sample exceedance probability of intervals as a function of interval duration for various values of T_L, T_u and S_c.

Such statistics are most useful when they can be used to estimate parameters, etc. for a clearly defined mathematical model for the process. For example, if the intervals between pulses were Poisson distributed, knowledge of the mean interval would completely specify the probability distribution of these intervals.

The first aspect of the data we will address is the question of whether the intervals between pulses (as defined in Fig. 6-1) form a renewal process, i.e., a process where the intervals are independent, identically distributed random variables (the Poisson process is a special case of a renewal process where the probability density function of the intervals between bursts is of the form $p(t) = \lambda e^{-\lambda t}$). The properties of such process are discussed in detail in various texts. [21] The tests most commonly used to check the consistency of the data with the hypothesis of a renewal process are;

(1) serial correlation coefficients: for large numbers of intervals, these are equivalent to the normalized auto correlation function, $\Phi(j)$, of the discrete process $\{x_1, x_2, \ldots, x_{n_o}\}$ where

16

$x_i \triangleq$ duration of the ith interval

$$\Phi(j) = \frac{E[(x_i - \bar{x})(x_{i+j} - \bar{x})]}{Var(x)} \qquad (VI-1)$$

For a renewal process $\Phi(j) = 0$ for $j \neq 0$.

(2) the spectrum of intervals: for large number of intervals, this is equivalent to the Fourier transform of $\Phi(j)$. The considerations involved in our previous discussion of spectral analysis apply in this case. For a renewal process, the spectrum of intervals is flat, i.e., a non-zero constant.

(3) contingency tables: these correspond to estimates of the joint density function of intervals that are j intervals apart; i.e., $p(x_{k+j}, x_i)$*. For a renewal process

$$p(x_{i+j}, x_i) = p_x(x_{i+j})\, p_x(x_i) \qquad (VI-2)$$

or alternatively

$$p(x_{i+j} \mid x_k) = p_x(x_{i+j}) \qquad (VI-3)$$

(4) conditional means: these correspond to the conditional expectation of an interval that is some number of intervals after a given interval, i.e.,

$$E(x_{i+j} \mid x_i) = \int_{o}^{\infty} x_{i+j}\, p(x_{i+j} \mid x_i)\, dx_{i+j} \qquad (VI-4)$$

For renewal processes, the expected value is independent of x_i, i.e.,

$$E(x_{i+j}) = E(x) \qquad (VI-5)$$

---

*This can of course be extended to triplets of intervals [e.g., $p(x_{i+j+k}, x_i, x_{i+j})$] and so on. In practice, this is hardly ever done because of the problem in obtaining adequate estimates.

An exact test for independence would involve showing that the joint density of all orders of intervals factors analogous to equations VI-2 on VI-3. This clearly is impossible to show in practice, and so one is generally content with examining the second order properties of the intervals (tests 1 and 2 above) and examining the properties of the joint density (tests 3 and 4) for rather small values of j. Our (rather limited) analysis to date has focused on the use of tests 3 and 4 (although in the near future results of applying the first two tests will be available).

In Figs. 6-2 and 6-3 we show a scattergram based on high noise level June data where each row is a plot of the sample conditional probability $p_s(x_{i+1} | x_i)$ where the darkness of the plotted point is proportional to $p_s(x_{i+1}, x_i)$ (if there were no intervals of value x_i followed by an interval of value x_{i+1}, no point is plotted). In Figs. 6-4 and 6-5 we plot the sample conditional mean interval, $E_s(x_{i+1} | x_i)$, as a function of x_i. The relatively small number of intervals means that we should expect relatively large statistical fluctuations in $p_s(\;.\;)$ and $E_s(\;.\;)$. From Figs. 6-4 and 6-5, it appears that the conditional mean interval is somewhat smaller than the (unconditional) mean interval for small lengths of the previous interval; this indicates that there is a slight tendency for short intervals to be followed by intervals that are shorter than the "average". From Figs. 6-2 and 6-3, it would appear that such a correlation does not arise from a case where the form of $p_x(x_{i+1} | x_i)$ is qualitatively different when x_i is small as opposed to when x_i is large. From Figs. 6-2 to 6-5 (and other results not shown here), it appears that the hypothesis that the data can modeled as a renewal process is not violently contradicted by the results of the tests utilized to date.

Thus, it appears useful to try to characterize the process of intervals in somewhat greater detail as a renewal process. Such a process can be completely described by a variety of probability functions for x, the length of the interval between bursts. The three that we shall consider here are:

(1) the probability density function p(x)

(2) the survivor function $R(x) \triangleq$ fraction of intervals greater than or equal to x (this function is analogous to the exceedance probability discussed earlier).

(3) the hazard function $H(x) \triangleq \frac{p(x)}{R(x)}$. The motivation for the use of this function (which is also known in other contexts as the failure rate, age-specific failure rate or force of mortality) is somewhat clearer if one notes that

$H(x)$ dx = probability of an interval duration in interval (x, x+dx) conditional on the interval duration being at least of length x

= probability of a pulse in the next dx seconds given that the last pulse was x seconds ago.

For a Poisson process,

$H(x) = \lambda \triangleq$ intensity or arrival rate of the process for all x.

These three functions are related as follows:

$$R(x) = \int_{x}^{\infty} p(u)du = \exp\left[- \int_{o}^{x} H(u)du \right] \qquad \text{(VI-6)}$$

In practice, we found the sample hazard function

$$H_s(x) \triangleq \frac{p_s(x)}{R_s(x)} \qquad \text{(VI-7)}$$

where $p_s(x)$ = sample density function

= fraction of intervals in range $(x - \frac{\delta}{2}, \ x + \frac{\delta}{2})$

where δ = binwidth of calculation

$R_s(x)$ = sample survivor function

= fraction of intervals $\geq$ x.

19

to be most useful in obtaining a model for $p(x)$ for small values of x while $R_s(x)$ is more useful when one considers a model of $p(x)$ for large values of x*.

In Figs. 6-6 and 6-7, we show $R_s(x)$ and $H_s(x)$ for some Florida ELF data processed with a variety of values of the parameters in Fig. 6-1. In Figs. 6-8 and 6-9 we show $H_s(x)$ and $p_s(x)$ for several different sets of data from Florida. Figures 6-6 to 6-9 are quite representative of the data analyzed to date. From such data we conclude that there the process of intervals between pulses in the wideband ELF process differs significantly from a Poisson process in that short intervals are more probable [as measured by $H_s(x)$] than larger intervals. However, the tails of probability distribution of intervals seem to be exponential, i. e., $R(x) \approx e^{-kx}$ for large x which is characteristics of a Poisson process. The empirical form of $H_s(x)$ does not appear to be fit particularly well over its entire range by common probability functions.

---

*This arises because $H_s(x)$ is quite sensitive to the statistical fluctuations that arise when there is a relatively small number of intervals in the range $(x - \frac{\delta}{2}, x + \frac{\delta}{2})$. As we shall see, long intervals, i. e., large values of x, are rather infrequent for the Florida ELF noise.

REFERENCES

1. Internal memorandum (not generally available).

2. J. Capon, P. Greenfield and R. Kolker, "Multidimensional Maximum-Likelihood Processing of a Large Aperture Seismic Array, " Proc. of IEEE, 55, 192-211, February 1967.

3. J. Cooley, P. Lewis and P. Welch, The Fast Fourier Transform Algorithm and Its Applications, IBM Research Paper RC-1743 (1967).

4. M. Balser and C. Wagner, "Observations of Earth-Ionosphere Cavity Resonances, " Nature, 188, 638-641, November 1960.

5. R. Blackman, Linear Data-Smoothing and Prediction in Theory and Practice, Reading, Mass: Addis -Wesley (1965).

6. M. Balser and C. Wagner, "Measurements of the Spectrum of Radio Noise from 50 to 100 Cycles Per Second, " J. Research NBS, 64D, 415-423, (1960).

7. M. Balser and C. A. Wagner, "Diurnal Power Variations of the Earth-Ionosphere Cavity Modes and Their Relationship to Worldwide Thunderstorm Activity, " J. Geophys. Res., 67, No. 2, 619-625, February 1962.

8. R. Gendrin and R. Stefand, "Magnetic Records Between 0.2 and 30 c/s, " AGARD Conference on Propagation of Radio Frequencies Below 300 kc/s, Munich, Germany, September 1962.

9. C. Polk and F. Fitchen, "Schumann Resonances of the Earth-Ionosphere Cavity-Extremely Low Frequency Reception at Kingston, R.I., " J. Res. NBS, 66D (Radio Prop.), No. 3, 313-318, (1962).

10. E. L. Maxwell, "Atmospheric Noise from 20 kHz to 30 kHz, " Radio Science, 2, 637-644, June 1967.

11. E. Maxwell and D. Stone, "Natural Noise Fields from 1 cps to 100 kc, " IEEE Trans. on Antennas and Propagation, 339-343, May 1963.

12. J. Galejs, "Schumann Resonances, " Radio Sciences, 69D, 1043-1054, August 1965.

13. T. Larsen, "High Latitude Investigations of Electromagnetic Phenomena in the Frequency Range 3-75 Hz, " Doctoral Thesis, University of Oslo, Oslo, Norway (1967).

14. "ELF Noise Measurements at Riverhead, Long Island, New York, " RCA Laboratories, Princeton, N.J., September, 1963.

15. A. Egland, et al, "Final Scientific Report (Task A) ELF and VLF Emissions in Northern Scandinavia, " Norwegian Institute of Cosmic Physics, Oslo, Norway, September 1966.

16. W. O. Schumann, "Uber Die Strahlungslosen Eigenschwingungen Einer Leitenden Kugel, Die Von Einer Luftschicht Und Einer Ionospharenhulle Umgeben Ist, " A. Naturforsch, 7a (1952).

17. P. Nelson, "Ionospheric Perturbations and Schumann Resonance Data, " Ph.D. Thesis, MIT Dept. of Geology and Geophysics (May 1967).

18. P. Beckmann, "Amplitude-Probability Distribution of Atmospheric Radio Noise, " Radio Science, 68D, 723 (June 1964).

19. K. Furutsu and T. Ishida, "On the Theory of Amplitude Distribution of Impulsive Random Noise, " J. of Applied Physics, 32, No. 7, 1206-1221, July 1961.

20. L. Remizou, et al., "Distribution of the Probabilities of Intervals Between Pulses of Atmospheric Noise, " Radiotekhnika i Elektronika 651-653 (1966).

21. D. Cox and P. Lewis, The Statistical Analysis of Series of Events London: Methuen & Co. (1966).

ANALOG RECORDER ○ → A/D → DIGITAL TAPE → POWER SPECTRUM

DIGITAL RECORDER ○

EQUALIZATION ← ○ ANTENNA TYPE

DIGITAL TAPE

APD
POWER DENSITY SPECTRUM
WAVEFORM ANALYSIS
BURST STATISTICS

3-66-8616(2)
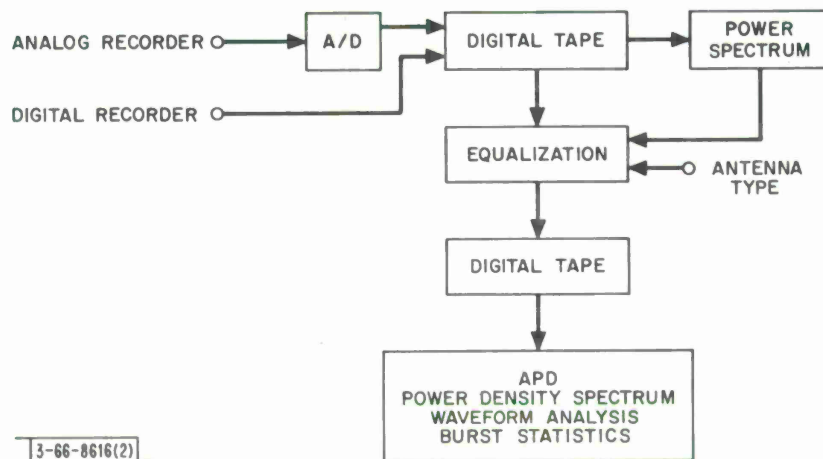
Fig. 2-1.   Block Diagram of Noise Processing.

18-6-8730

T_S = TIME DURATION OF A SEGMENT IN SECONDS
ω_o = FILTER CENTER FREQUENCY

FILTER RESPONSE (dB)

$\frac{4}{\pi}(\omega - \omega_o)T_S$
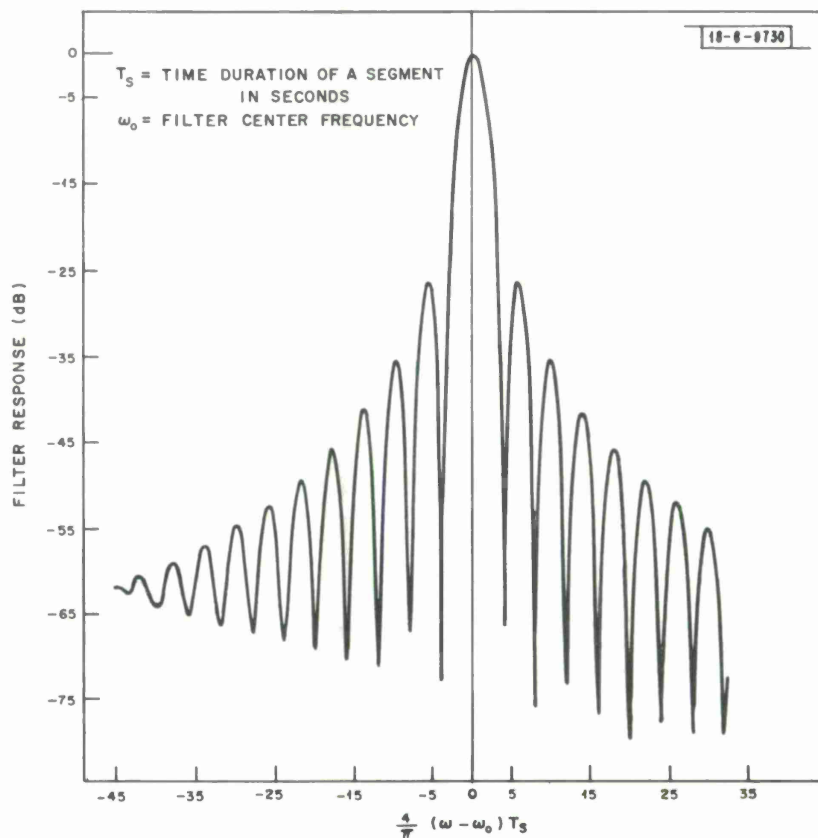
Fig. 2-2.   Spectral Analysis Filter Frequency Response.
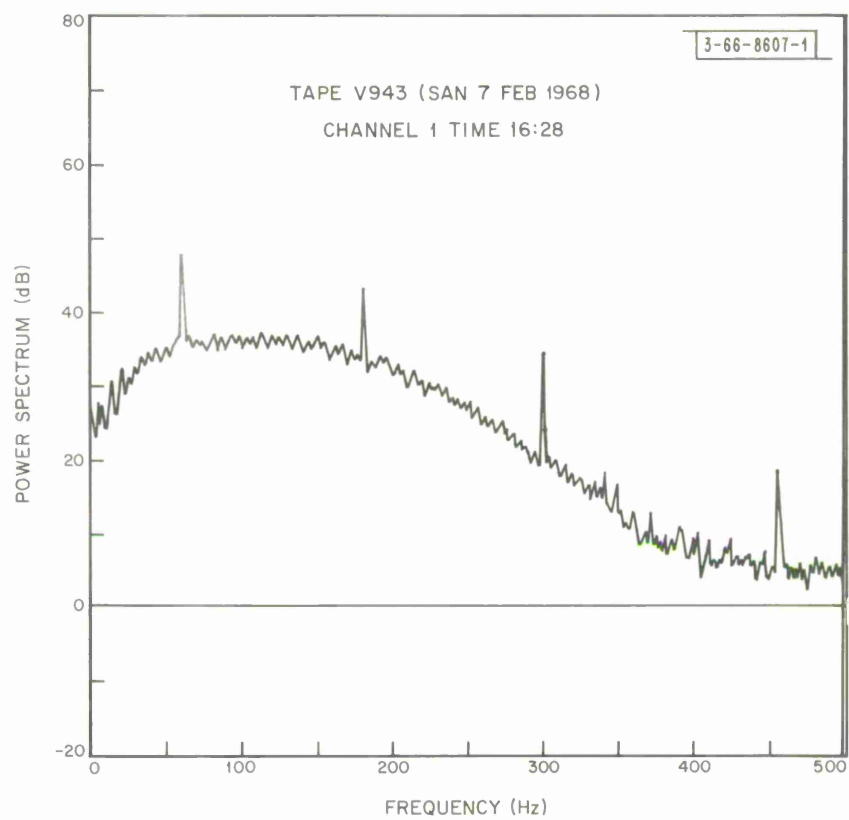
Fig. 2-3. Power Density Spectrum of ELF Data Before Compensation.
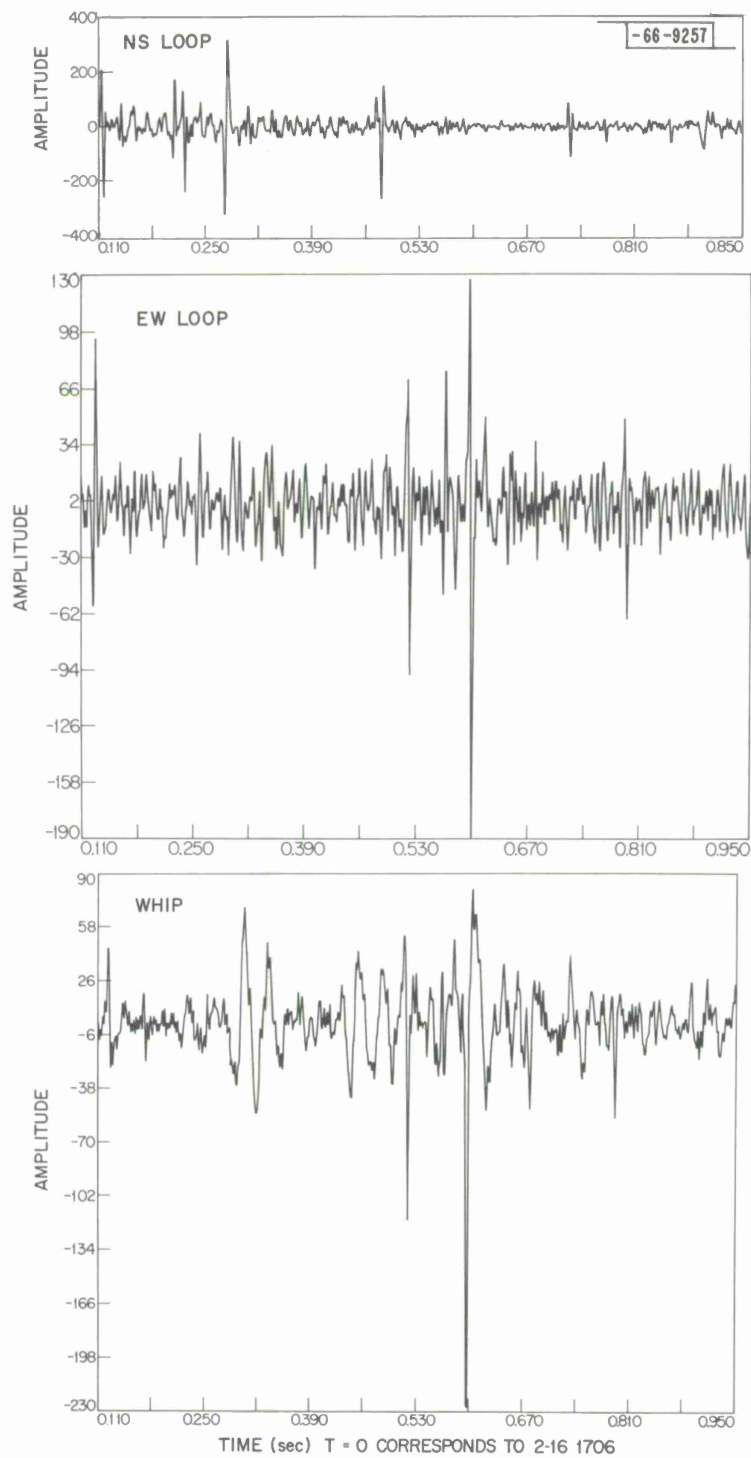
Fig. 3-1.   ELF Waveforms Recorded in Florida (Feb. 1968).
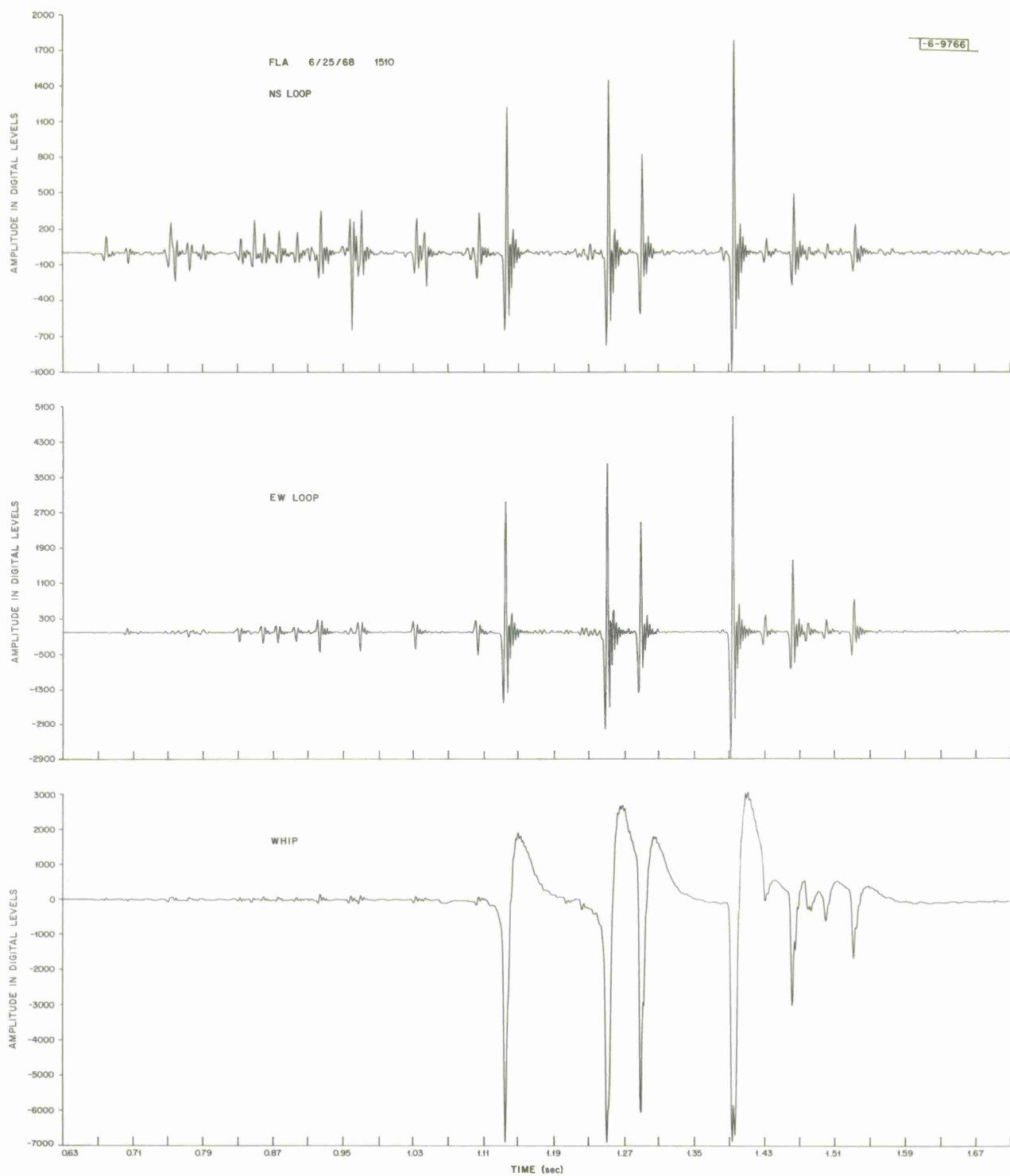
Fig. 3-2. ELF Waveforms Recorded in Florida (June 1968).

26
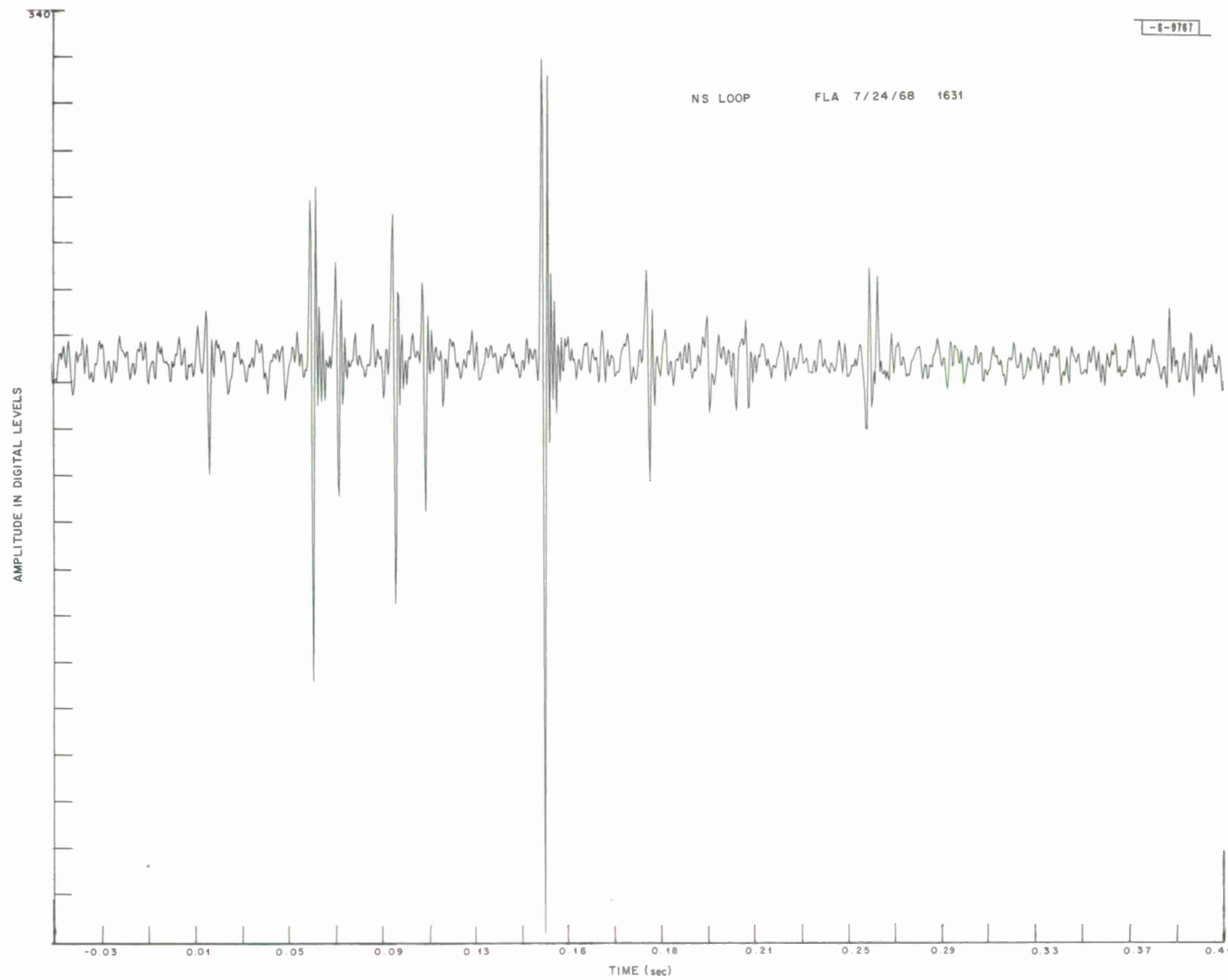
Fig. 3-3.   ELF Waveforms Recorded in Florida (July 1968).

NS LOOP   FLA 7/24/68   1631

AMPLITUDE IN DIGITAL LEVELS

TIME (sec)

27

WIDEBAND NOISE: 10–300 Hz

3-Hz BANDWIDTH AT 200 Hz

3-Hz BANDWIDTH AT 100 Hz

3-Hz BANDWIDTH AT 50 Hz

3-Hz BANDWIDTH AT 20 Hz

1/2 SEC

TYPICAL ELF ATMOSPHERIC NOISE
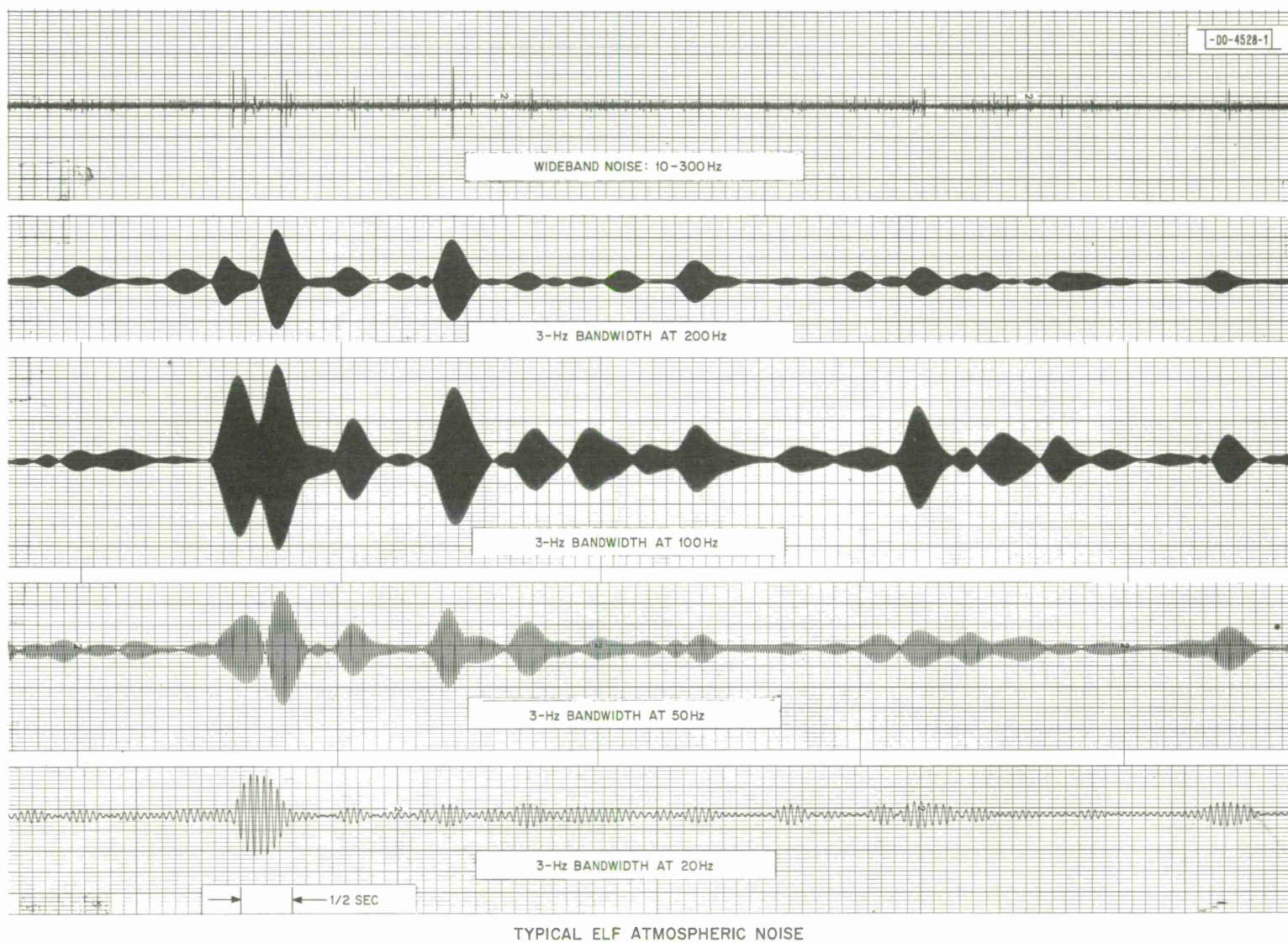
Fig. 3-4.   Wideband and Narrow Band ELF Noise from Florida (Feb. 1968).
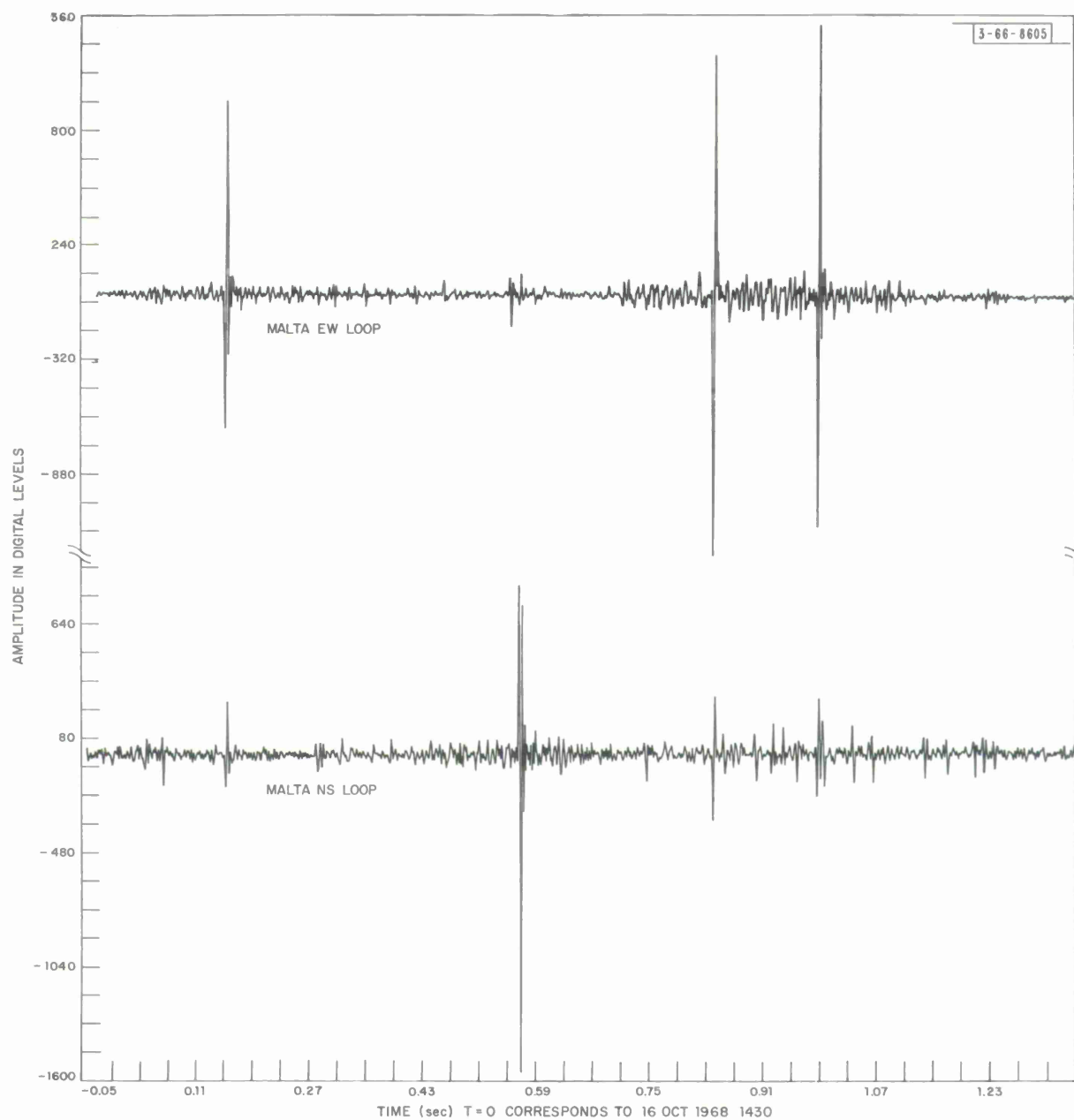
Fig. 3-5.   ELF Waveforms Recorded in Malta (Oct. 1968).

29
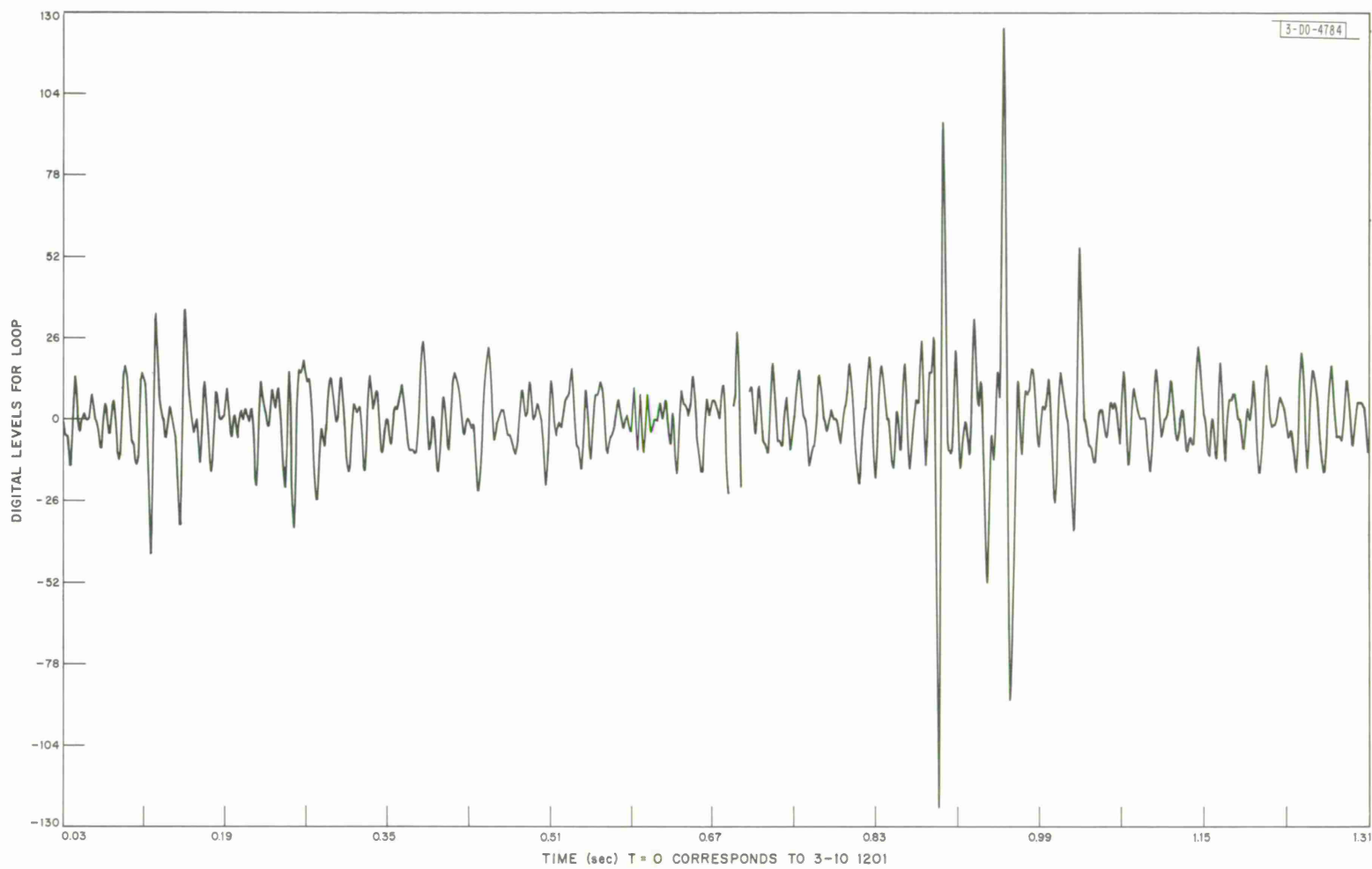
Fig. 3-6.   ELF Waveforms Recorded in New Hampshire (March 1968).

30
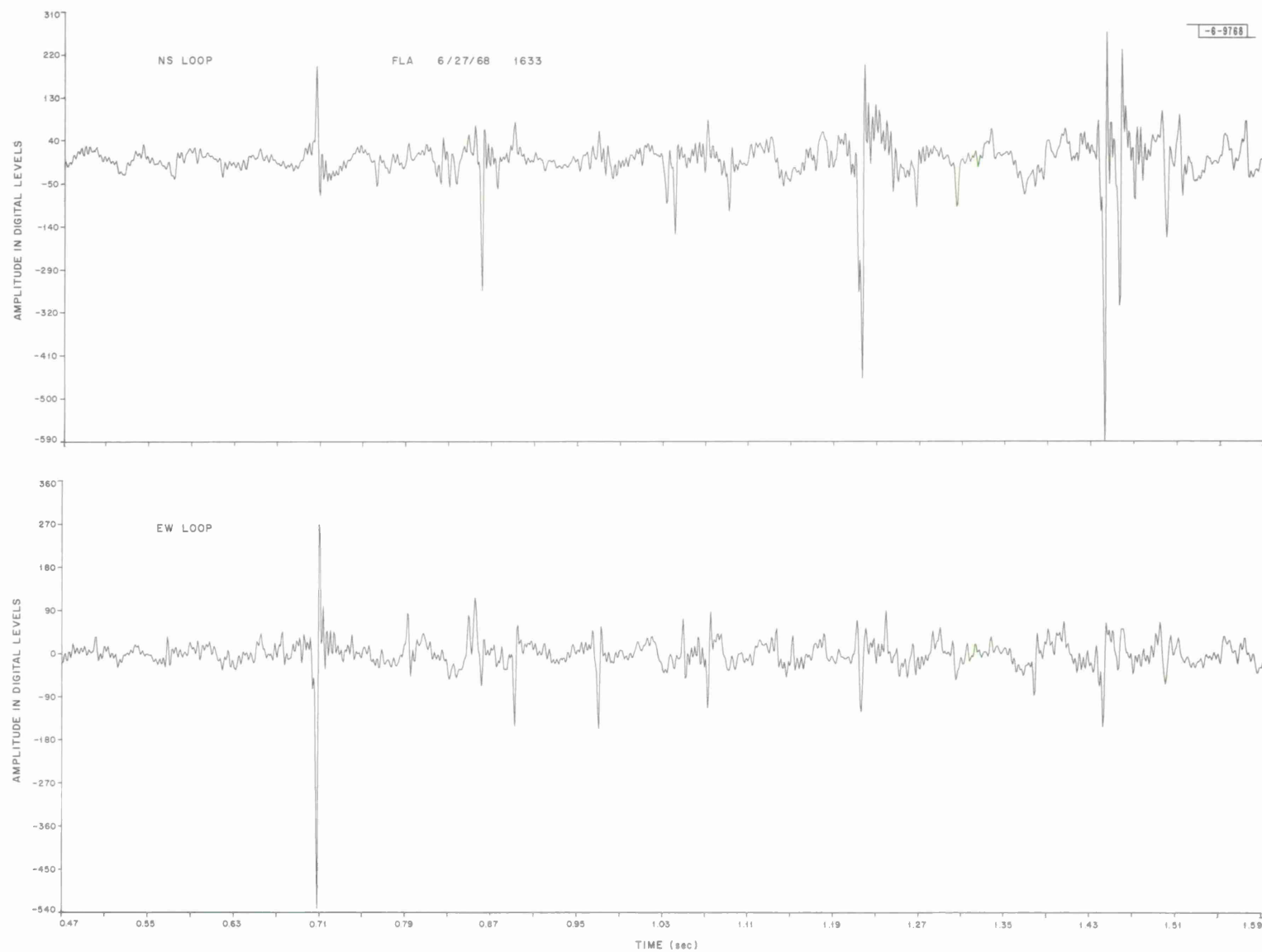
Fig. 3-7.   ELF Waveforms Recorded in Florida after Compensation (June 1968).
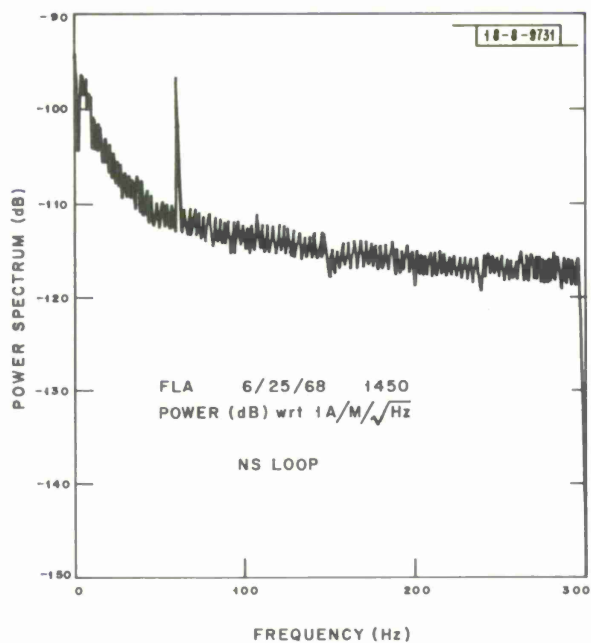
Fig. 4-1. Wideband Power Density Spectrum for Florida Data (June 1968).
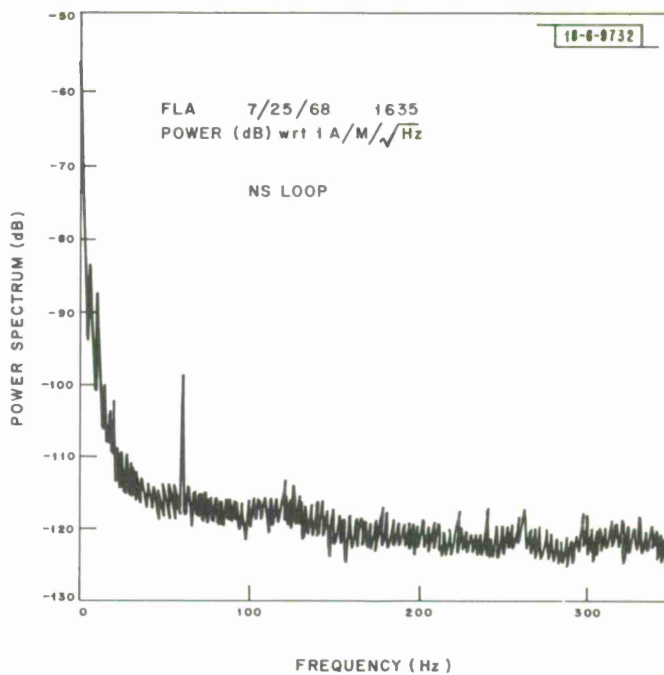
Fig. 4-2. Wideband Power Density Spectrum for Florida Data (July 1968).
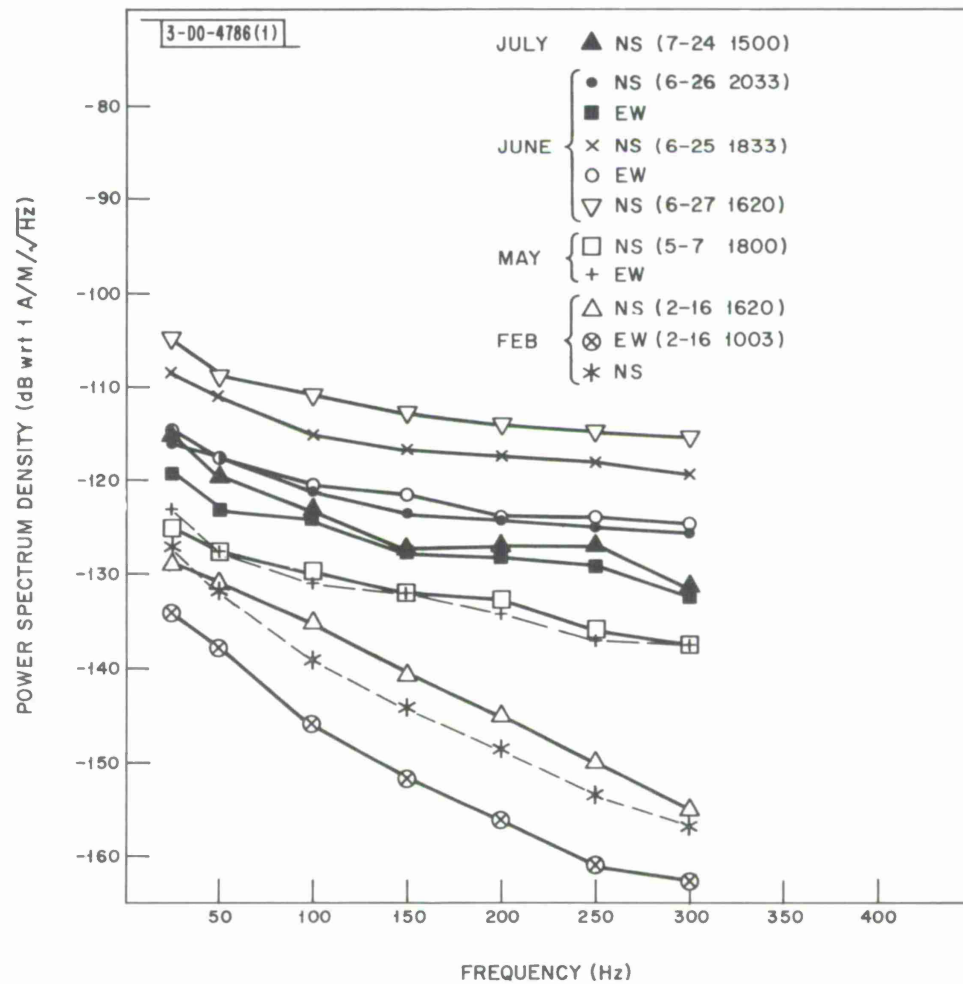
Fig. 4-3. Wideband Power Density Spectrum for Florida Data (Feb., May, June, July 1968).
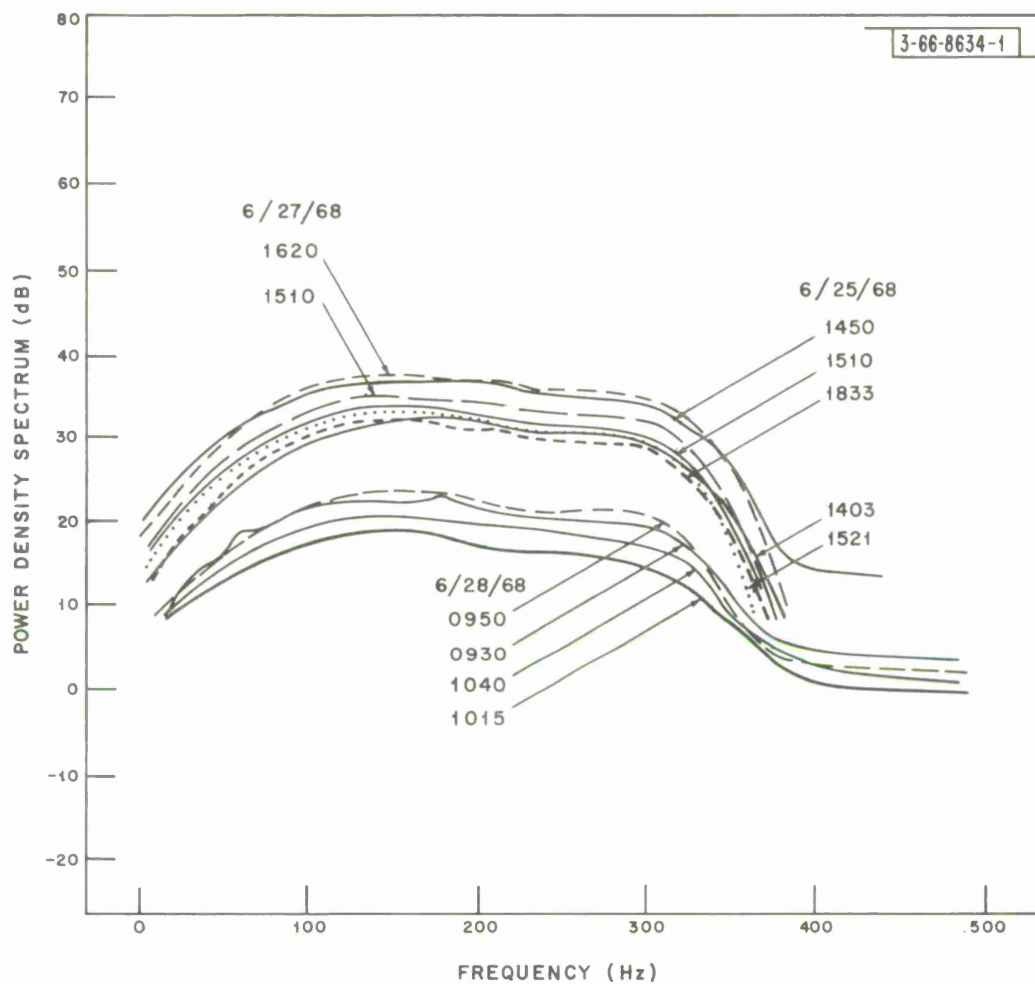
Fig. 4-4. Diurnal Variations in Power Density Spectrum in Florida
(June 1968).
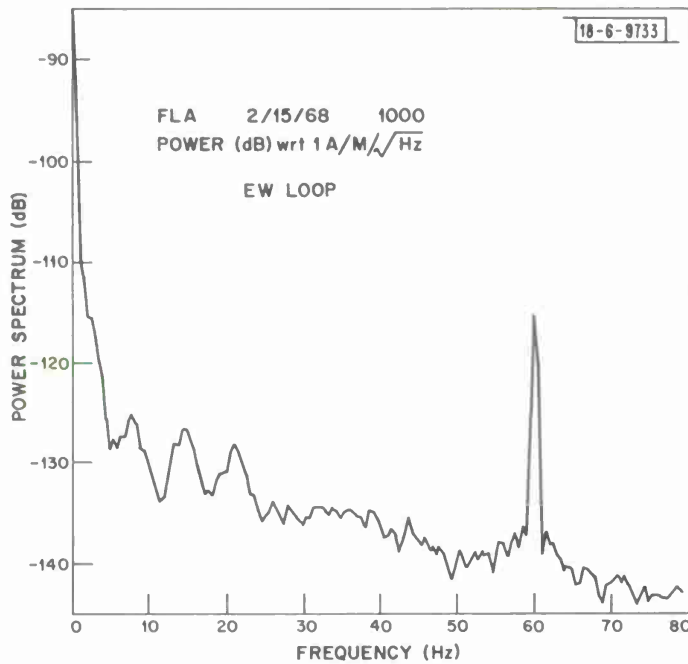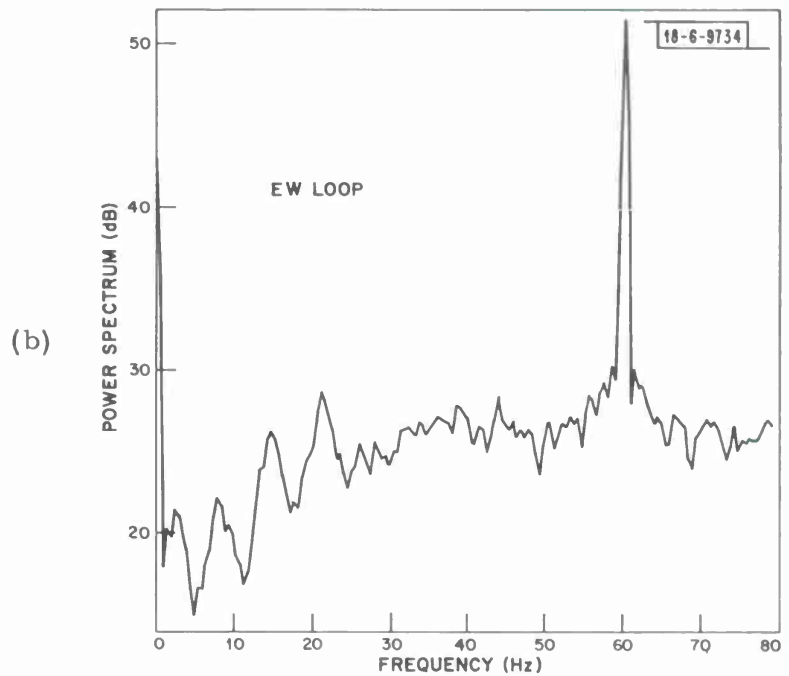
Fig. 4-5.   Shumann Resonances in Florida (Feb. 1968).

35
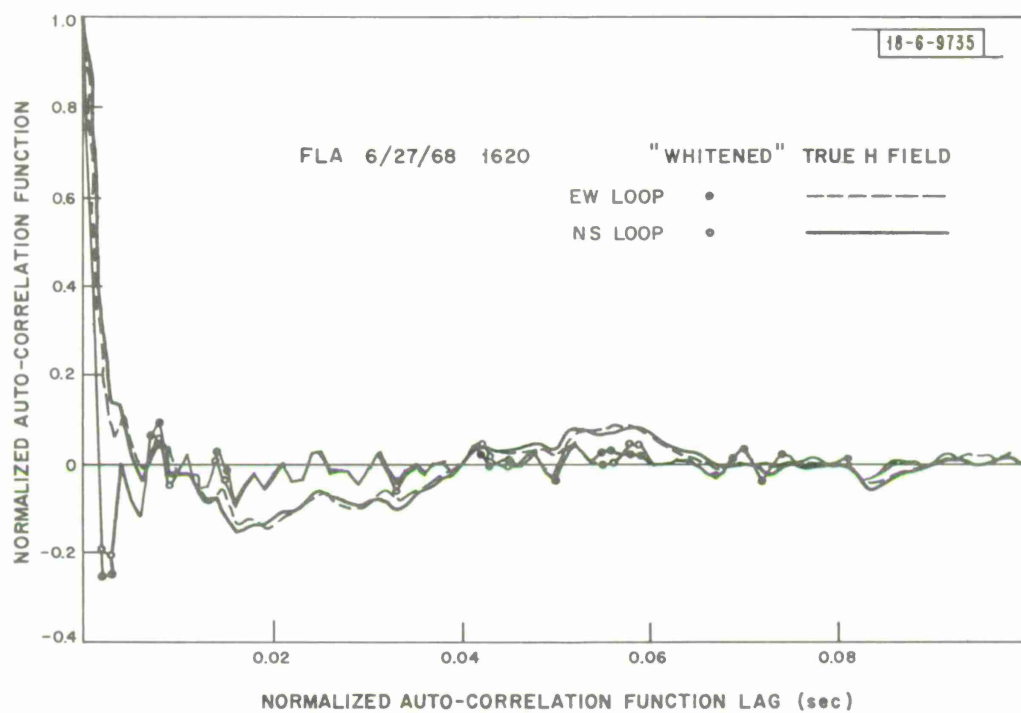
Fig. 4-6. Normalized Auto-correlation Function for Florida Data.
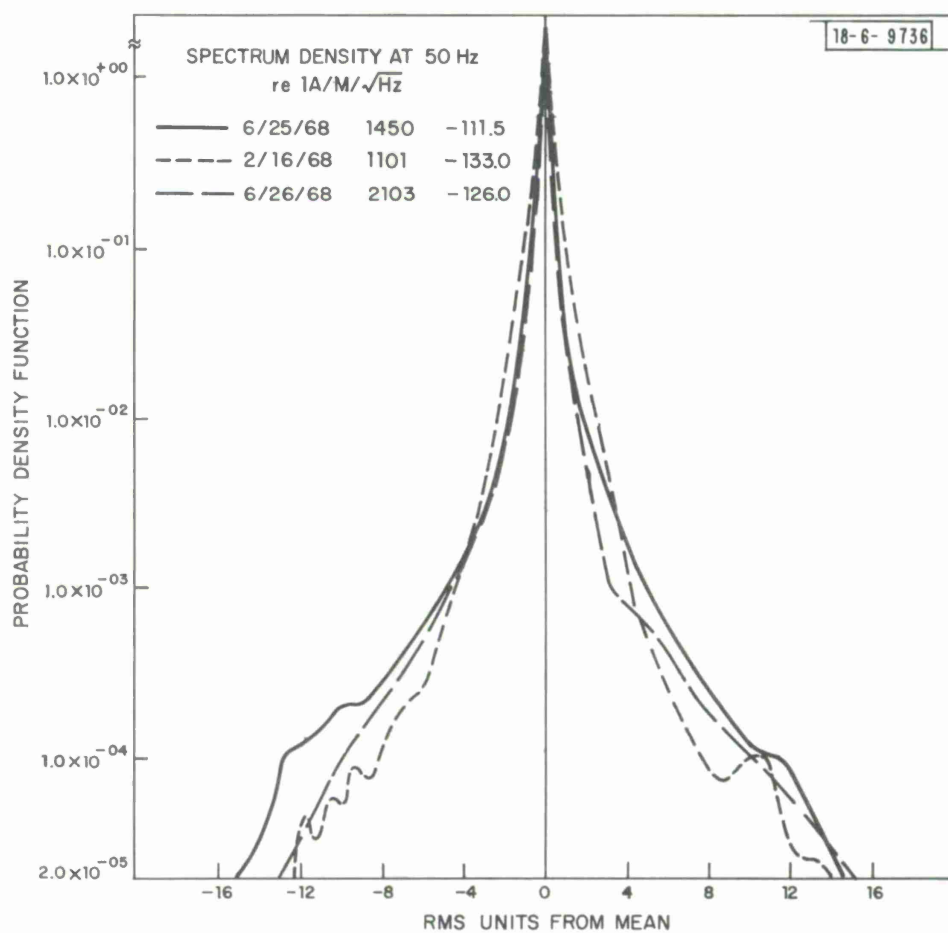
Fig. 5-1. Probability Density Function for Florida Data (Feb., June 1968).
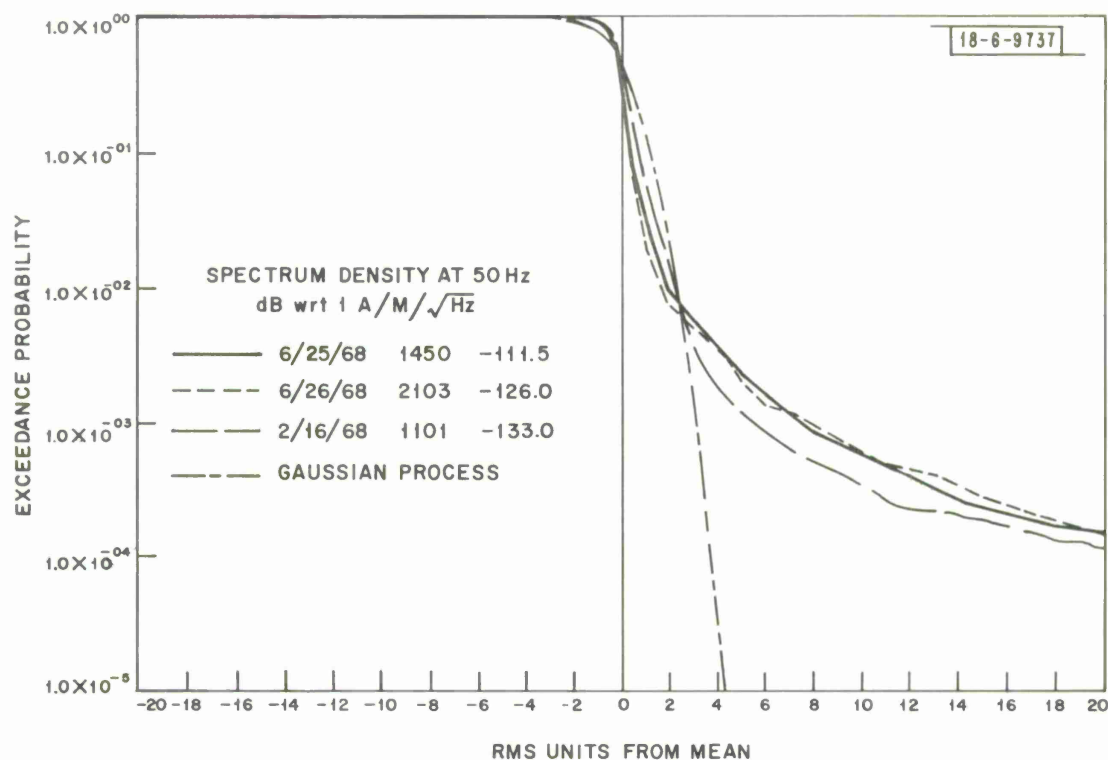
Fig. 5-2.   Exceedance Probability Function for Florida Data
(Feb., June 1968).
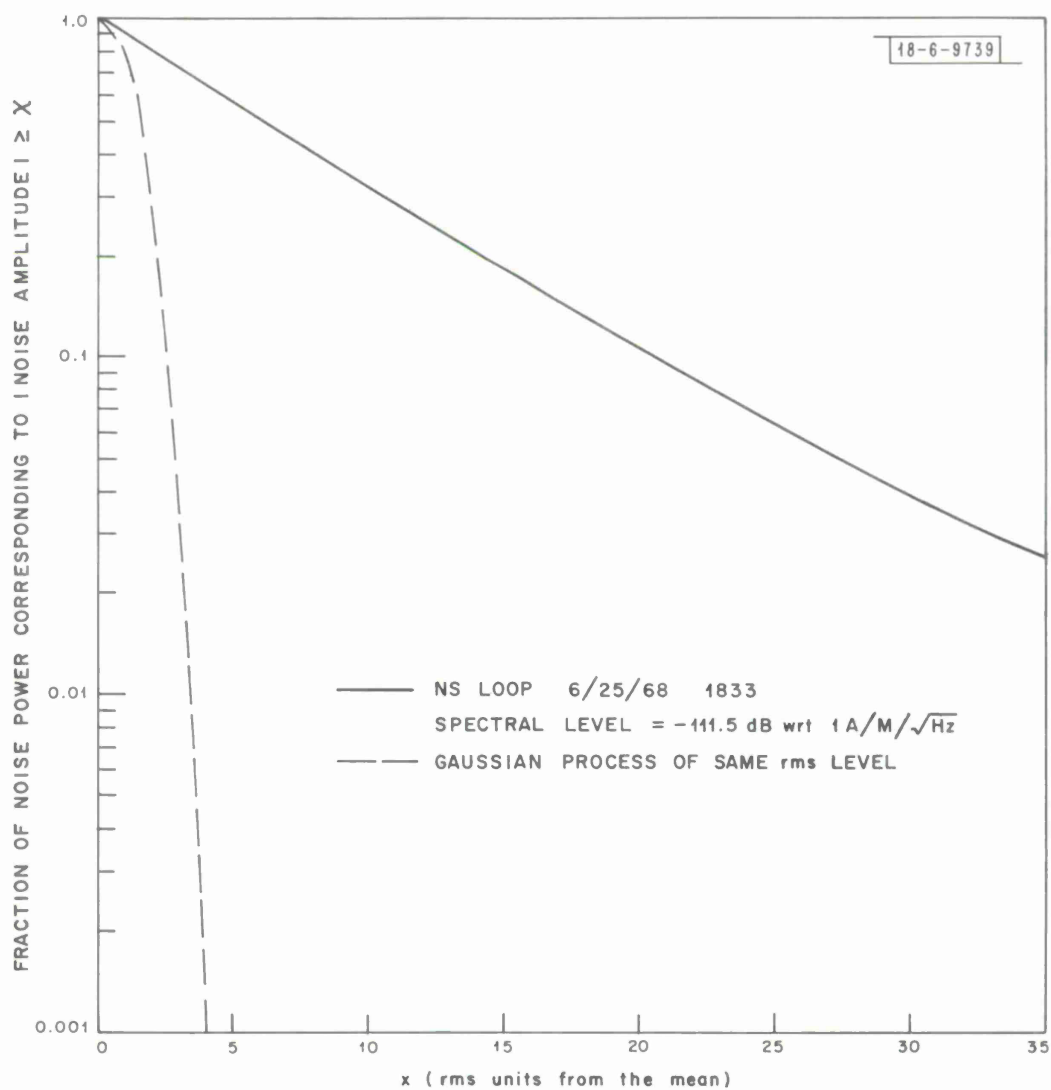
Fig. 5-3. Noise Power Exceedance Fraction versus Noise Amplitude
for Florida Data (June 1968).

39
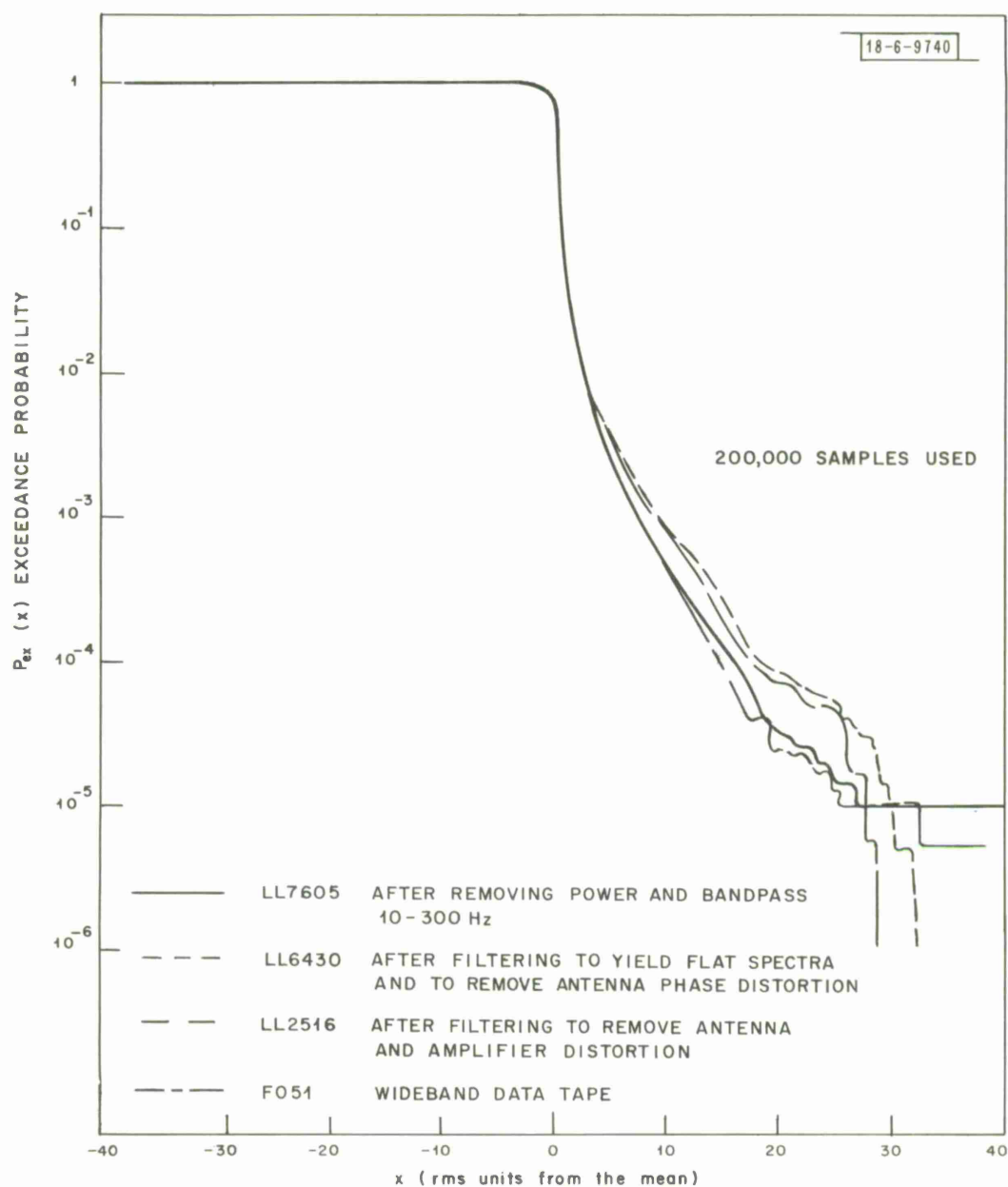
Fig. 5-4. Exceedance Probability for Florida Data for Various
Compensations (June 1968).
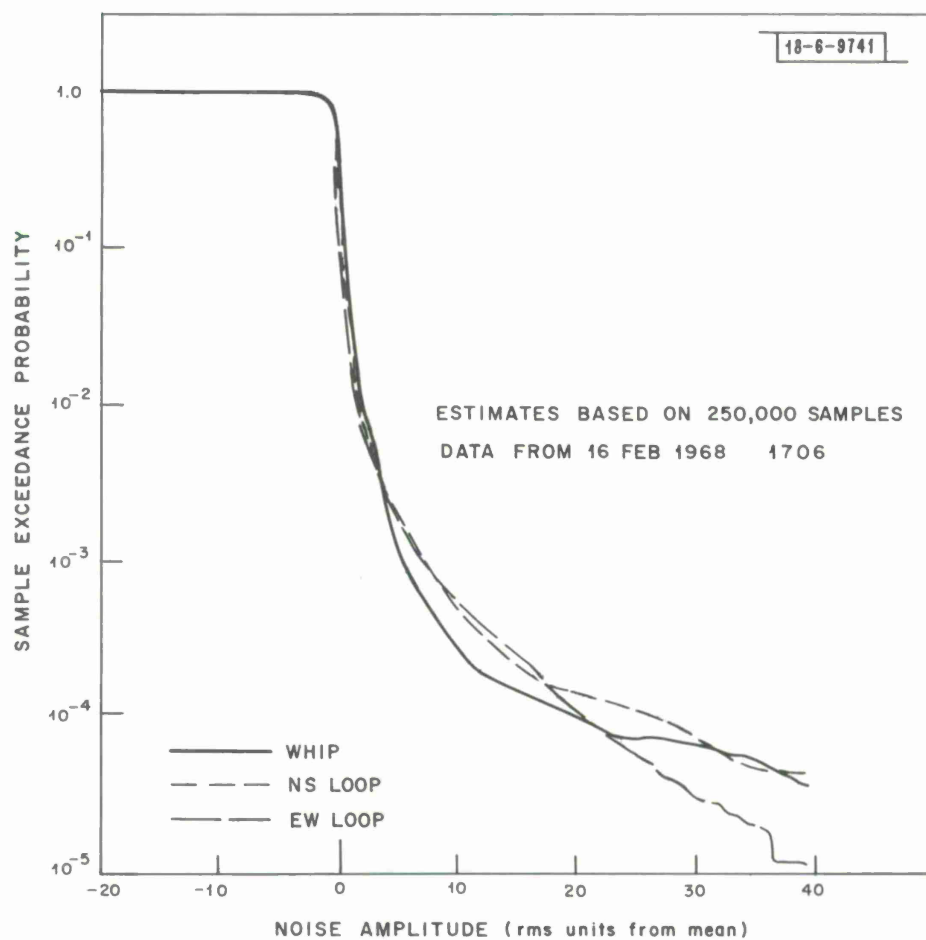
Fig. 5-5. Exceedance Probability for Various Sensors in Florida (Feb. 1968).

41

3-00-4796-1

EXCEEDANCE PROBABILITY

1.0

0.1

0.01

0.001

0.0001

0.00001

	PB	RMS
▲	0–350	41.9
+	2–250	35.8
△	2–200	31.4
O	2–150	23.5
□	2–100	13.6
×	2–60	6.2
■	90–110	1.7

(all based on 2×10^5 samples)

	PB	RMS
✳	0–350	45.4

(based on 1.4×10^5 samples)

6-26 1833
REDUCED GAIN: NS LOOP

SPECTRA LEVEL
AT 50 Hz = –111.5 db wrt $1A/M/\sqrt{Hz}$

0   10   20   30   35

RMS UNITS FROM MEAN
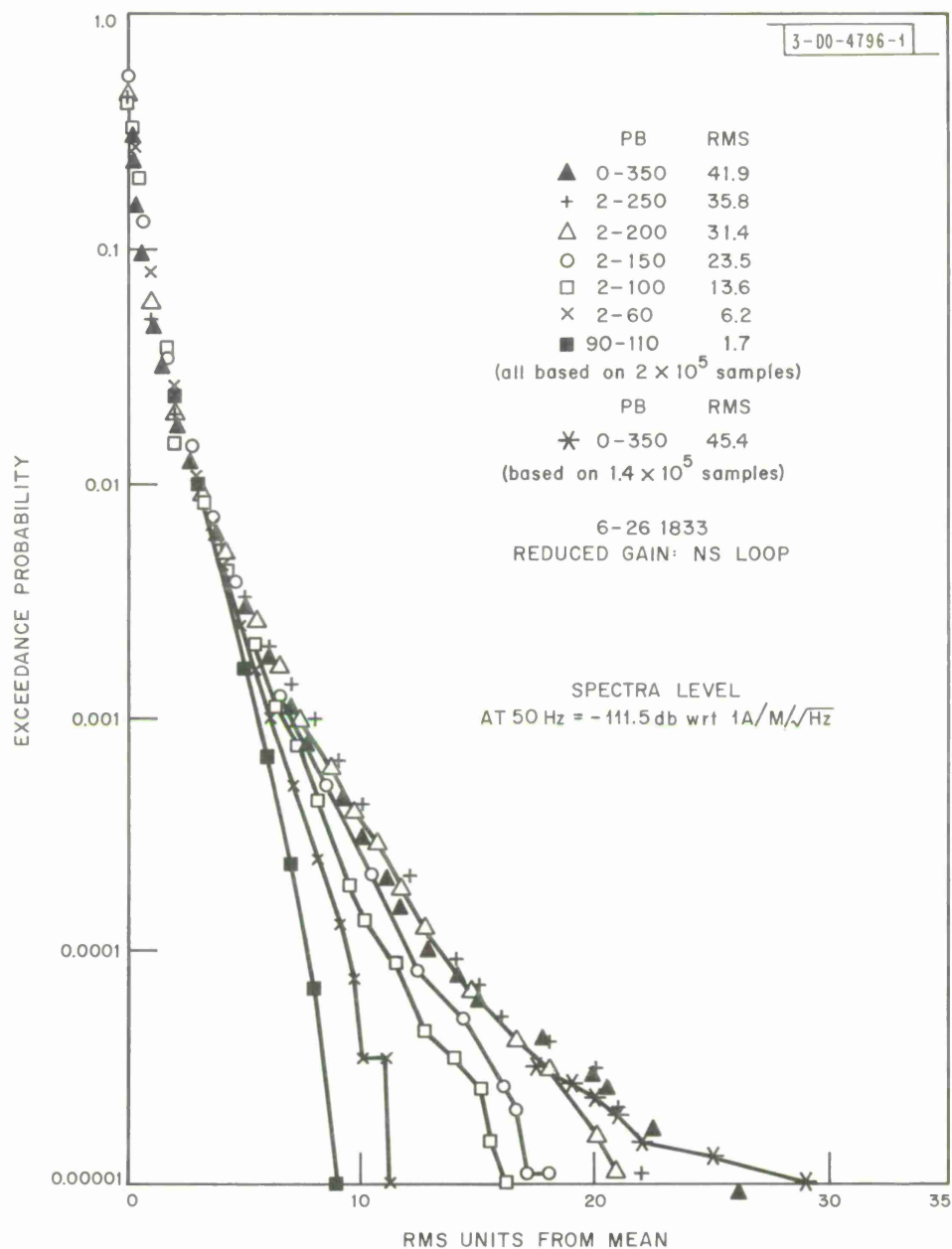
Fig. 5-6.   Exceedance Probability as a Function of Bandwidth for Florida Data (June 1968).

42
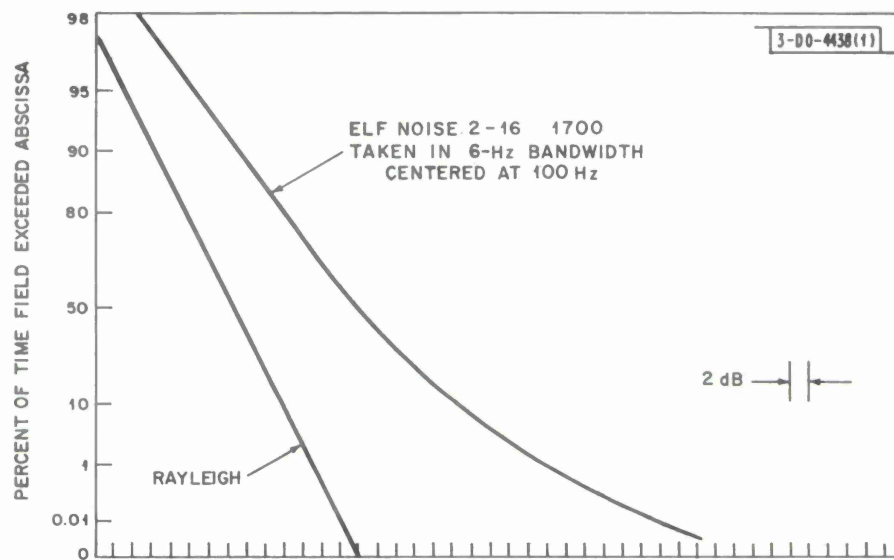
Fig. 5-7.   Exceedance Probability for Narrow Band Envelope of Florida Data (Feb. 1968).
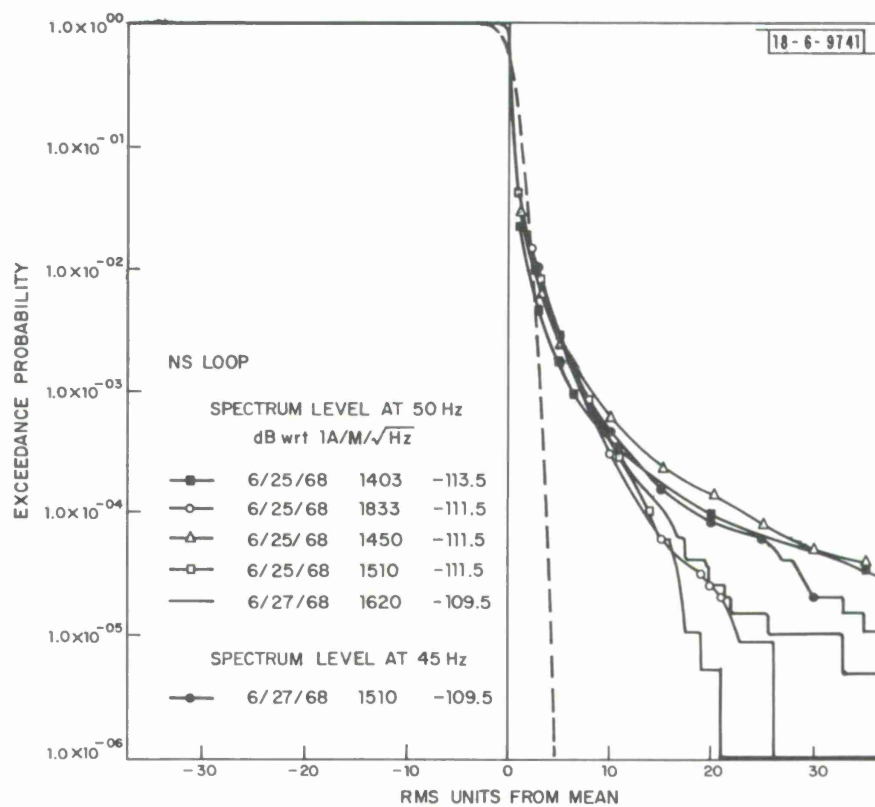
Fig. 5-8.   Exceedance Probability for Various Data Recorded in Florida During June 1968.
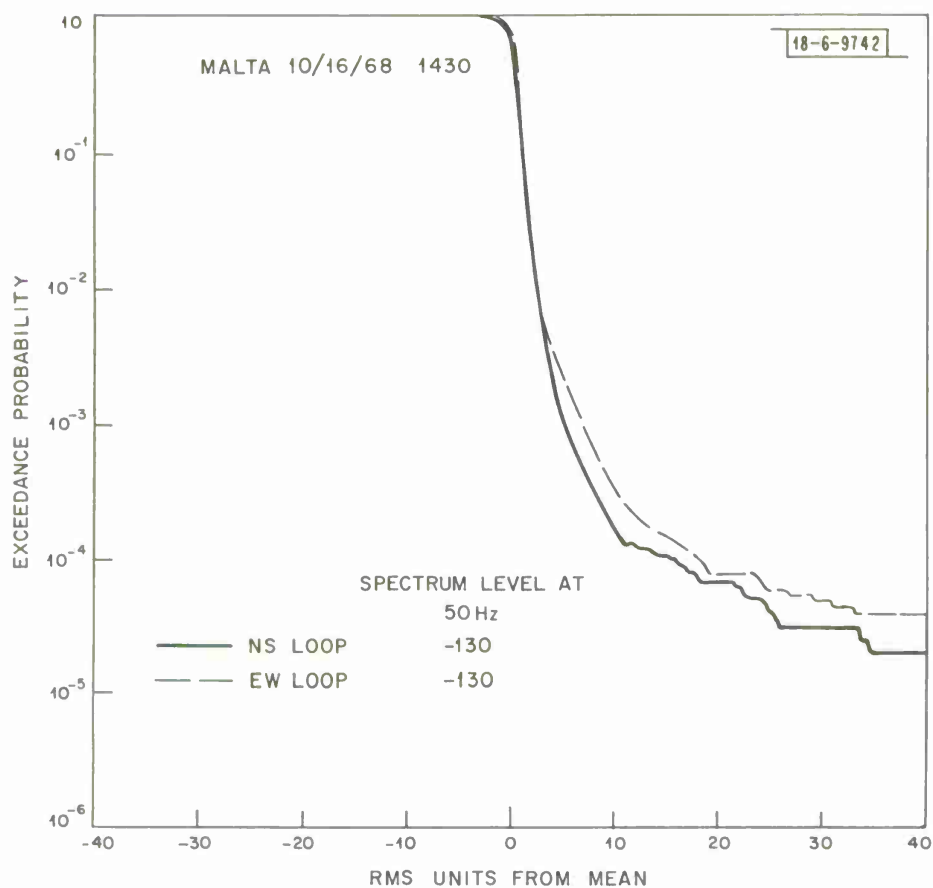
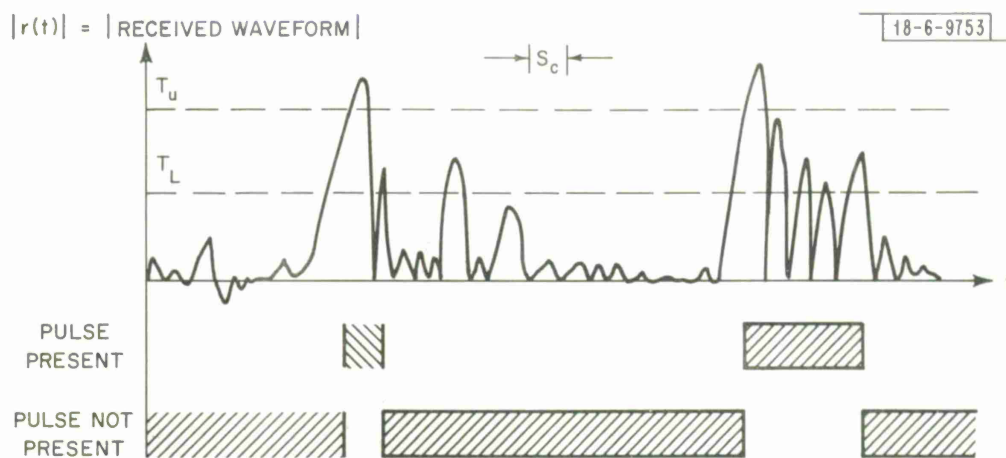Fig. 5-9.   Exceedance Probability for Malta Data (Oct. 1968).
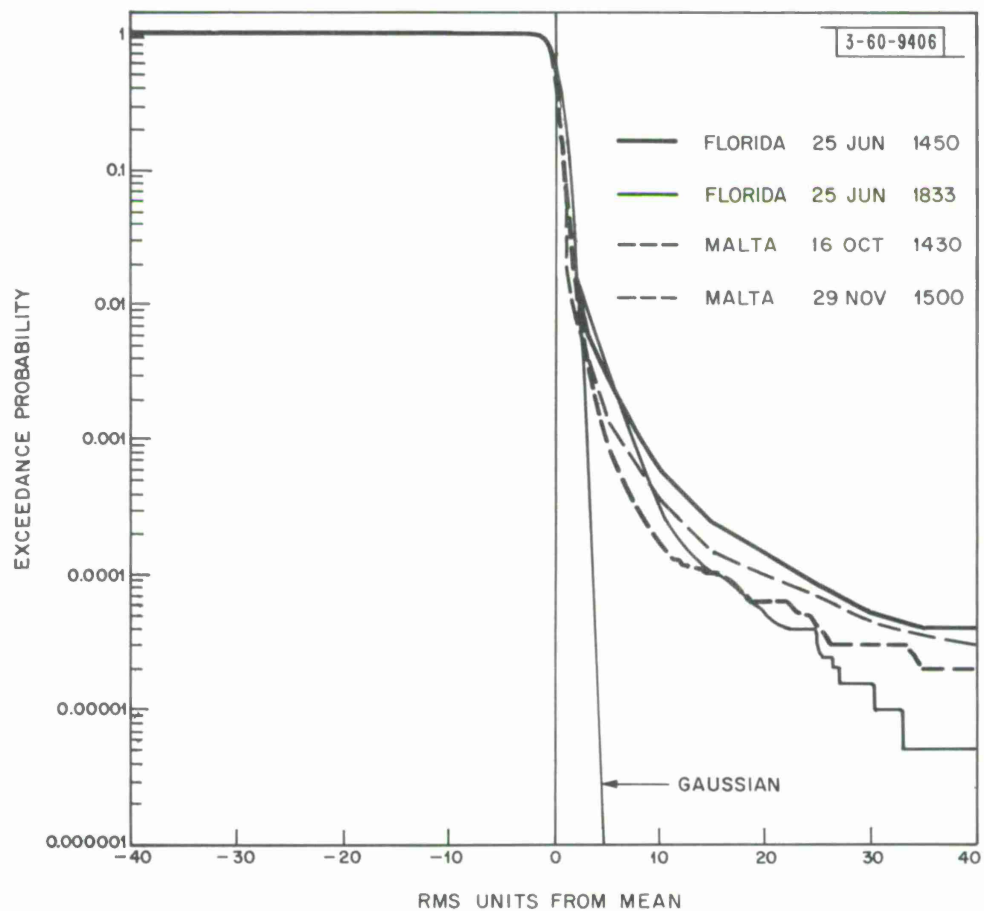
Fig. 5-10. Comparison of Florida and Malta Exceedance Probabilities.

45

$|r(t)| = |$ RECEIVED WAVEFORM $|$

18-6-9753

T_u

T_L

$\rightarrow |S_c| \leftarrow$

t

PULSE
PRESENT

PULSE NOT
PRESENT

(1) Pulse "begins" when $|r(t)| \geqslant$ threshold T_u

(2) Pulse "continues" until $|r(t)| <$ threshold T_L for a
continuous period of S_c seconds.

where

$r(t) \triangleq$ received waveform.

Fig. 6-1. Criteria Defining "Beginning" and "End" of Wideband ELF
Noise Pulse (Florida, June 1968).
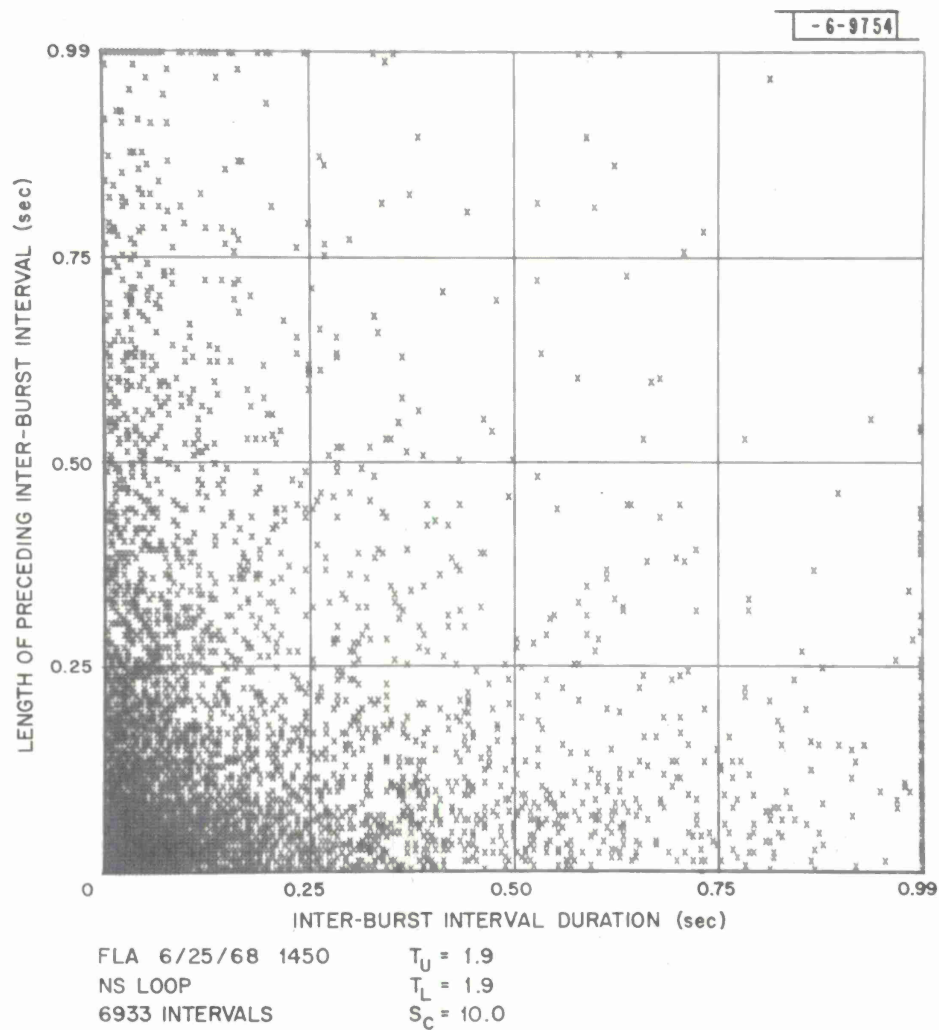
Fig. 6-2. Scattergram for Inter-Burst Interval Distributions (Florida, June 1968).

47
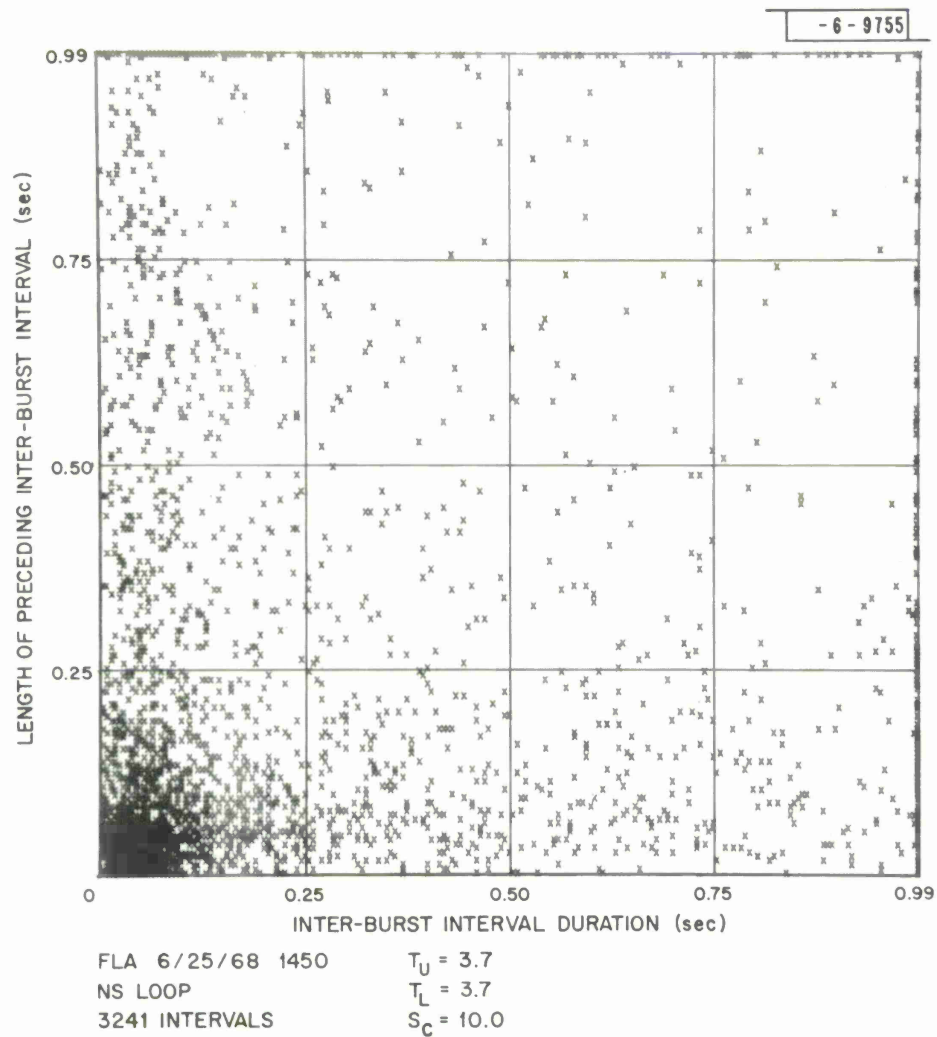
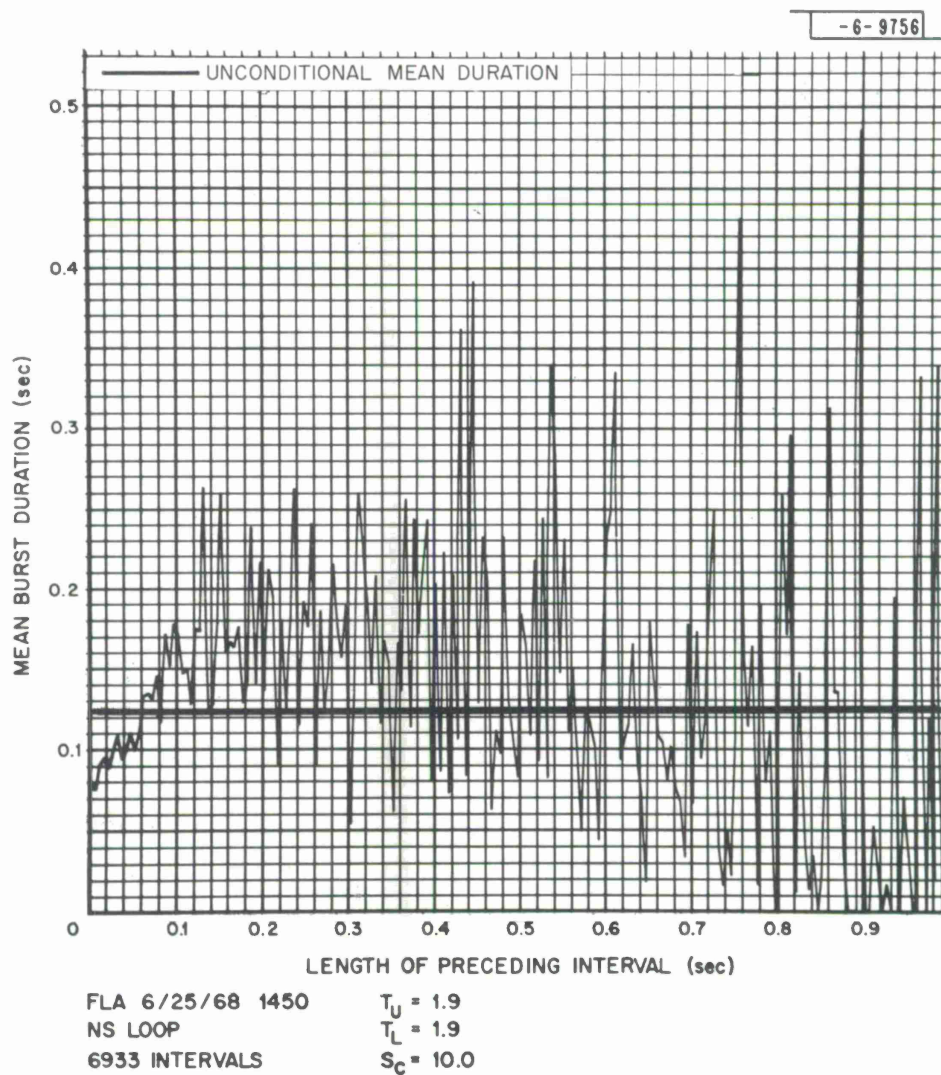Fig. 6-3.   Scattergram for Inter-Burst Interval Distributions
(Florida, June 1968).

Fig. 6-4. Conditional Mean of Inter-Burst Interval (Florida, June 1968).
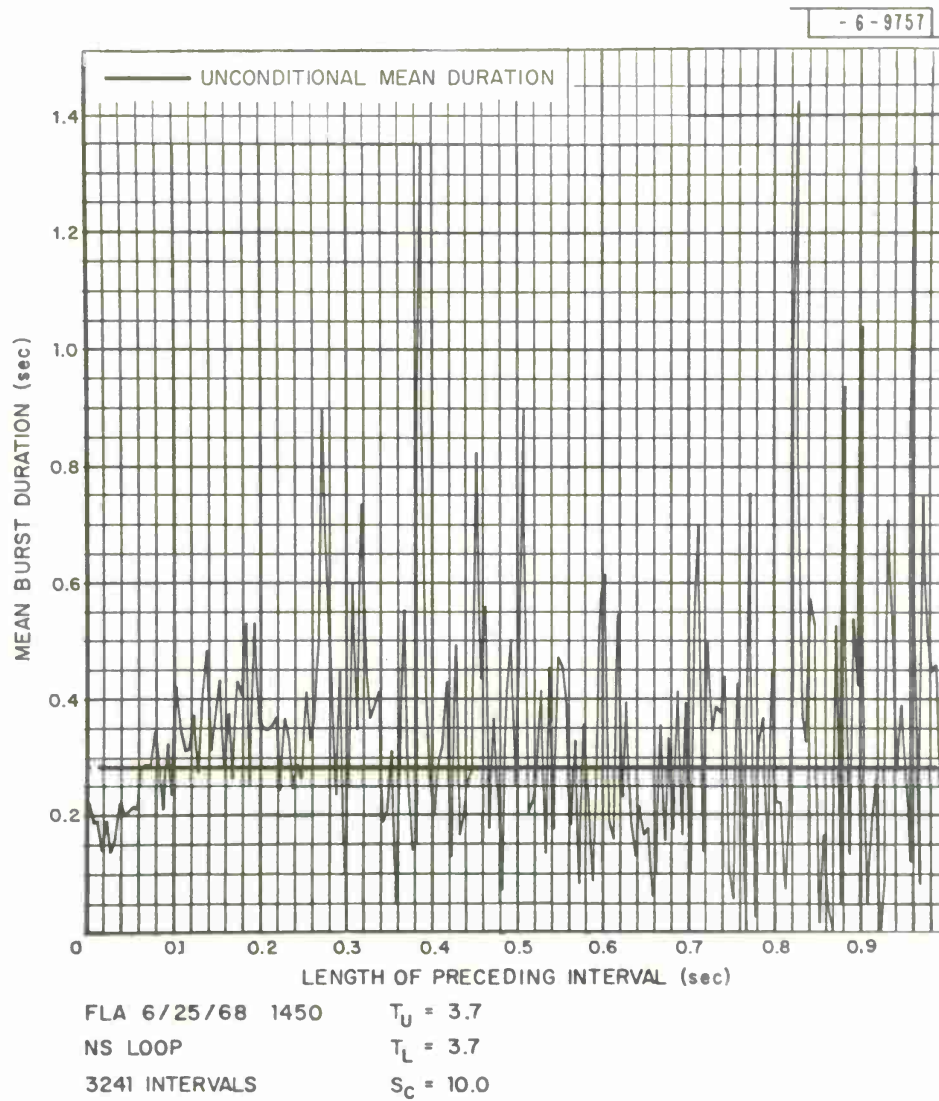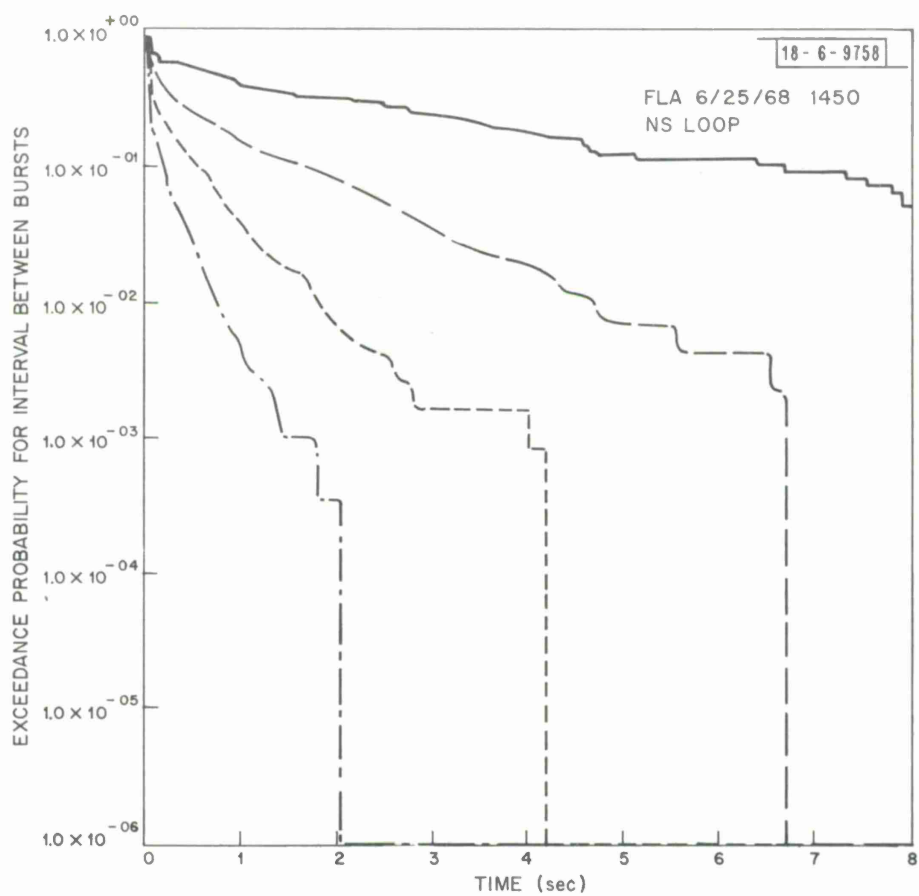
Fig. 6-5.   Conditional Mean of Inter-Burst Interval (Florida, June 1968).

	RMS	T_{UPPER}	T_{LOWER}	SC	NO. BURSTS
————	51.7	14.3	14.3	2.0	94
— — —	51.7	7.1	7.1	2.0	400
- - - -	51.7	3.6	3.6	2.0	1168
—·—·—	51.7	1.8	1.8	2.0	2846

Fig. 6-6. Exceedance Probability of Inter-Burst Interval for Various Criteria (Florida, June 1968).
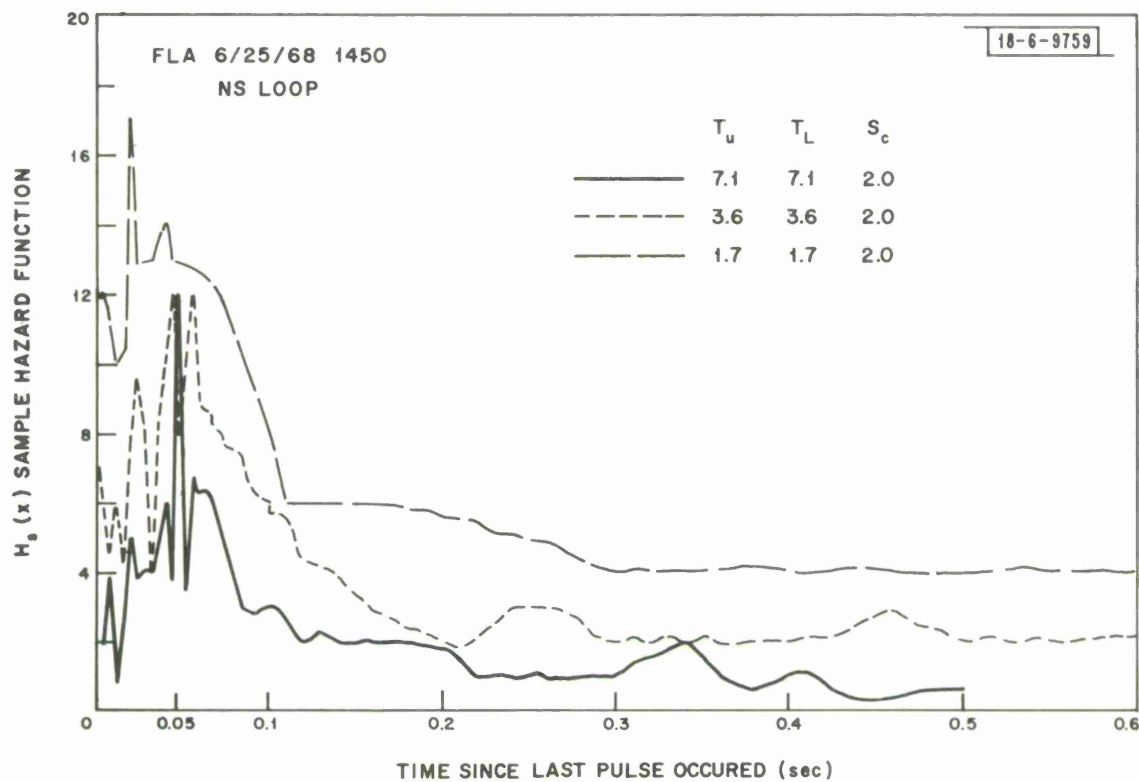
51

Fig. 6-7. Hazard Function of Inter-Burst Interval for Various Criteria (Florida, June 1968).
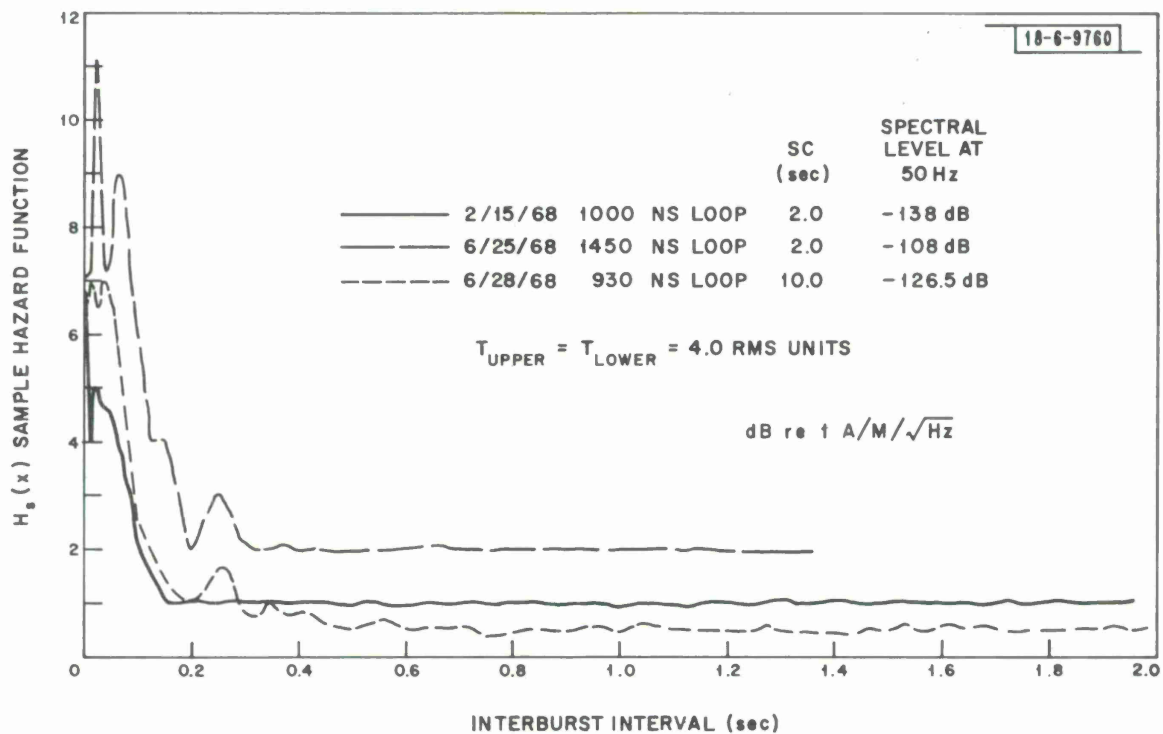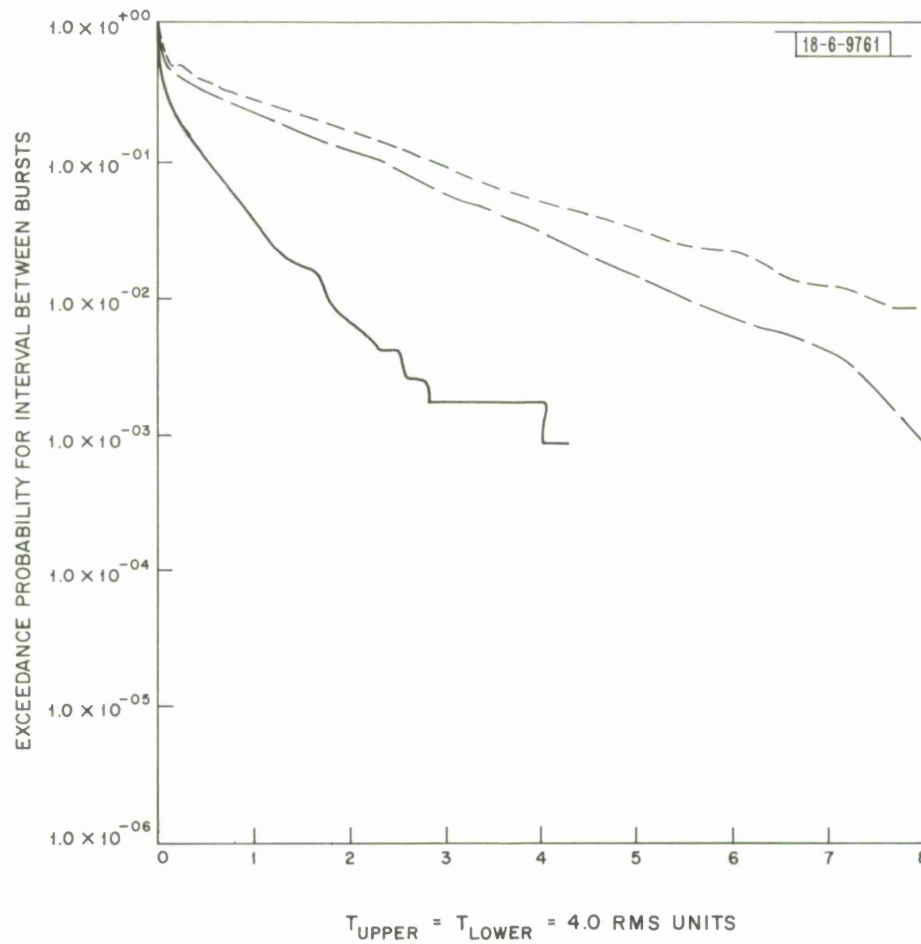
Fig. 6-8. Hazard Function of Interburst Interval for Various Florida Data.

Fig. 6-9. Exceedance Probability of Inter-Burst Interval for Various Florida Data.

DOCUMENT CONTROL DATA – R&D		
(Security classification of title, body of abstract and indexing annotation must be entered when the overall report is classified)		

1. ORIGINATING ACTIVITY *(Corporate author)*	2a. REPORT SECURITY CLASSIFICATION
Lincoln Laboratory, M.I.T.	Unclassified
	2b. GROUP
	None

3. REPORT TITLE

Preliminary Analysis of ELF Noise

4. DESCRIPTIVE NOTES *(Type of report and inclusive dates)*

Technical Note

5. AUTHOR(S) *(Last name, first name, initial)*

Evans, James E.

6. REPORT DATE	7a. TOTAL NO. OF PAGES	7b. NO. OF REFS
26 March 1969	60	21

8a. CONTRACT OR GRANT NO.	9a. ORIGINATOR'S REPORT NUMBER(S)
AF 19(628)-5167	
b. PROJECT NO.	Technical Note 1969-18
1508A	
c.	9b. OTHER REPORT NO(S) *(Any other numbers that may be assigned this report)*
d.	ESD-TR-69-67

10. AVAILABILITY/LIMITATION NOTICES

This document has been approved for public release and sale; its distribution is unlimited.

11. SUPPLEMENTARY NOTES	12. SPONSORING MILITARY ACTIVITY
None	U.S. Navy

13. ABSTRACT

Preliminary results of analyzing extremely low frequency (ELF) electromagnetic noise recorded in Florida and Malta are presented. The results include wideband waveforms, power density spectra, amplitude probability distributions and probability distributions for the duration of the interval between noise bursts. The distinctly non-Gaussian nature of the noise is demonstrated in a variety of ways.

14. KEY WORDS

ELF noise	amplitude distributions	signal-to-noise ratio
power spectra	Gaussian noise	Navy Communications
waveforms		